Ionisation-with-Excitation Calculations for Electron-Impact Helium Collisions within the S-Wave Model

Thomas Ross
Supervised by Professor Igor Bray

Declaration

I declare that the writings and results presented herein are, to the best of my knowledge, products of my own efforts, except where it has been explicitly acknowledged to be the work of others.

Thomas Ross, November 21, 2022.

Abstract

The application of the convergent close-coupling (CCC) method to the task of calculating total cross sections for electron-impact ionisation-with-excitation of helium, within the s-wave model, has been re-examined after disagreement was found with benchmark calculations using the propagating exterior complex scaling (PECS) method. The cause of the discrepancy has been identified, and demonstrated, to be the occurrence of mixed target states used in the CCC method, resulting from the intersection of the continuum ionised-without-excitation spectrum with the discrete doubly-excited and continuum ionised-with-excitation spectrum. Approaches to obtaining pure target states, and alternatively, to extracting accurate cross sections from the mixed target states have been put forward.

Acknowledgements

This work was supported by resources provided by the Pawsey Supercomputing Research Centre with funding from the Australian Government and the Government of Western Australia.

I wish to acknowledge my supervisor, Prof. Igor Bray, for his invaluable assistance in the conducting of this research; and both Prof. Bray and Dr. Brendan McGann for their patience and support - without which, I would not have been able to complete this research. I would also like to express my deep gratitude to Prof. Bray for his guidance, and his ceaseless encouragement.

Contents

List of Figures

List of Tables

List of Abbreviations

TCS: total cross section

SDCS: single-differential cross section

DDCS: double-differential cross section

TDCS: triple-differential cross section

TICS: total ionisation cross section

TIECS: total ionisation-with-excitation cross section; alternatively written as TICS-with-excitation

CCC: convergent close-coupling

CCC(N): convergent close-coupling calculation performed with N one-electron basis states

CCC(C, N): convergent close-coupling calculation performed with C core states and N one-electron basis states

CCC(C, N, λ): convergent close-coupling calculation performed with C core states, and N one-electron basis states with exponential fall-off parameter λ

ECS: exterior complex scaling

PECS: propagating exterior complex scaling

List of Notation

$\|\varphi_i\rangle$	Laguerre basis states
$\hat{A}$	anti-symmetriser operator
$\hat{P}_{i,j}$	pairwise exchange operators
$\hat{H}_T$	target Hamiltonian operator
$\hat{K}_m$	target electron kinetic operators
$\hat{V}_m$	target electron potential operators
$\hat{V}_{m,n}$	target electron-electron potential operators
$\hat{H}_{T,e}$	target Hamiltonian operator, restricted to one target electron
$\|\phi_i\rangle$	one-electron atomic orbitals
$\|\chi_i\rangle$	one-electron spin orbitals
$\|\chi_{[a_1,\ldots,a_n]}\rangle$	Slater determinants
$\|\Phi_n\rangle$ / ϵ_n	target (states / energies)
$\|\Phi_n^{(N)}\rangle$ / $\epsilon_n^{(N)}$	target (pseudostates / pseudoenergies), calculated with N one-electron basis states
$\|\Phi_n^{(C,N)}\rangle$ / $\epsilon_n^{(C,N)}$	target (pseudostates / pseudoenergies), calculated with C core states, and N one-electron basis states
$\hat{I}_T$	target states projection operator
$\hat{I}_T^{(N)}$	target pseudostates projection operator, calculated with N one-electron basis states
$\|\mathbf{k}_\alpha\rangle$ / $\frac{1}{2}k_\alpha^2$	projectile (states / energies), taking the form of continuum waves
$\hat{H}$	total Hamiltonian operator
$\hat{K}_0$	projectile electron kinetic operator
$\hat{V}_0$	projectile electron-nuclei potential operator
$\hat{V}_{0,m}$	projectile electron-target electron potential operators
$\|\Psi\rangle$	total wavefunction
E	total energy
$\|\psi\rangle$	unsymmetrised total wavefunction
$\|F_n^{(N)}\rangle$	multichannel weight functions, calculated with N one-electron basis states
$\|\Psi^{(N)}\rangle$ / $\|\psi^{(N)}\rangle$	multichannel-expanded (total wavefunction / unsymmetrised total wavefunction)

$\hat{H}_A$ asymptotic Hamiltonian operator, which is unbounded

$\hat{V}$ anti-symmetrised potential operator, which is bounded

$|\Phi_\alpha \mathbf{k}_\alpha\rangle$ / ε_α asymptotic (states / energies)

$|\Phi_{n_\alpha}^{(N)} \mathbf{k}_\alpha\rangle$ / $\varepsilon_\alpha^{(N)}$ asymptotic (pseudostates / pseudoenergies), calculated with N one-electron basis states

$\hat{T}$ the $\hat{T}$ operator

$\hat{K}$ the $\hat{K}$ operator

k_n on-shell projectile momenta

$f_{\alpha,\beta}$ scattering amplitudes, equivalently:

$$
\begin{aligned}
&= f_{\alpha,\beta}(\mathbf{k}_\alpha, \mathbf{k}_\beta) \\
&= \langle \mathbf{k}_\alpha \Phi_\alpha | \hat{V} | \Psi_\beta \rangle \\
&= \langle \mathbf{k}_\alpha \Phi_\alpha | \hat{T} | \Phi_\beta \mathbf{k}_\beta \rangle
\end{aligned}
$$

$f_i^{(N)}$ elastic scattering amplitudes, calculated with N one-electron basis states

$f_{f,i}^{(N)}$ discrete excitation scattering amplitudes, calculated with N one-electron basis states

$f_{\alpha,i}^{(N)}$ (unsymmetrised) ionisation scattering amplitudes, calculated with N one-electron basis states

$F_{\alpha,i}^{(N)}$ anti-symmetrised ionisation scattering amplitudes, calculated with N one-electron basis states

$\sigma_{\alpha,\beta}$ partial cross sections, equivalently:

$$
\begin{aligned}
&= \sigma_{\alpha,\beta}(\mathbf{k}_\alpha, \mathbf{k}_\beta) \\
&= \frac{k_\alpha}{k_\beta} |f_{\alpha,\beta}|^2 \\
&= \frac{k_\alpha}{k_\beta} |\langle \mathbf{k}_\alpha \Phi_\alpha | \hat{T} | \Phi_\beta \mathbf{k}_\beta \rangle|^2
\end{aligned}
$$

$\sigma_{\mathrm{T};i}^{(N)}$ total cross section for a given initial asymptotic state, calculated with N one-electron basis states

$\sigma_{\mathrm{I};i}^{(N)}$ total ionisation cross section for a given initial asymptotic state, calculated with N one-electron basis states

$\sigma_{\mathrm{I};n_f,i}^{(N)}$ ionisation cross section for given final and initial asymptotic states, calculated with N one-electron basis states

1 Introduction

1.1 Helium Atom

The helium atom consists of two electrons bound electromagnetically to a nucleus containing two protons and, restricting our attention to stable isotopes, either one (helium-3) or two (helium-4) neutrons. As the helium atom is light, it's (non-excited) quantum states are well defined by the following quantum numbers:

- S: total spin,
- L: orbital angular momentum,
- J: total angular momentum,

and can be compactly written with the term symbol ${}^{2S+1}L_J$, where $2S+1$ is the spin multiplicity, in accordance with the LS-coupling scheme. A specific electron configuration of the helium atom can be prepended to the term symbol when desired, being written in the form $n_1\ell_1 n_2\ell_2\,{}^{2S+1}L_J$, where n_1, n_2 are the principal quantum numbers, and ℓ_1, ℓ_2 are the orbital angular momentum quantum numbers for each electron. In the context of the S-wave model, we consider only the quantum states of the helium atom with $L = 0$: the singlet state ${}^1\mathrm{S}_0$, and the triplet state ${}^3\mathrm{S}_1$.

1.2 Electron-Impact Helium Scattering Processes

The impact of an electron projectile on a helium target can lead to a number of different scattering processes:

$$
\begin{aligned}
\mathrm{e}^- + \mathrm{He} &\rightarrow \mathrm{e}^- + \mathrm{He} && \text{(elastic)} \\
&\rightarrow \mathrm{e}^- + \mathrm{He}^{'} && \text{(single-excitation)} \\
&\rightarrow \mathrm{e}^- + \mathrm{He}^{''} && \text{(double-excitation)} \\
&\rightarrow 2\mathrm{e}^- + \mathrm{He}^{+} && \text{(ionisation-without-excitation)} \\
&\rightarrow 2\mathrm{e}^- + \mathrm{He}^{+'} && \text{(ionisation-with-excitation)} \\
&\rightarrow 3\mathrm{e}^- + \mathrm{He}^{++} && \text{(double-ionisation / breakup).}
\end{aligned}
$$

Helium also exhibits the phenomena of auto-ionisation, in which a doubly-excited helium state may spontaneously eject one electron:

$$
\begin{aligned}
\mathrm{He}^{''} &\rightarrow \mathrm{e}^- + \mathrm{He}^{+} && \text{(auto-ionisation-without-excitation)} \\
&\rightarrow \mathrm{e}^- + \mathrm{He}^{+'} && \text{(auto-ionisation-with-excitation).}
\end{aligned}
$$

The resulting helium ion may be in the ground state or an excited state, subject to the constraint of energy conservation. The interference between the discrete, doubly-excited states of helium and the unbounded, continuum states of the auto-ionised system is non-trivial and has significant consequences for the double-excitation scattering process. The treatment of auto-ionising states, and an analysis on their interference with the continuum states, is provided by Fano [1].

1.3 Theoretical Review

The field of computational atomic collision theory has been subject to rapid progress during the past few decades, with the increasing capability of computational hardware and software, and the development of new and extant techniques and methods. Notably, the Convergent Close-Coupling (CCC) method, which was intially developed to model the scattering processes of an electron projectile on a hydrogen target [2], has been established as both numerically tractable and accurate while retaining the property of being a unitary formulation. Proven capable of modelling elastic scattering and discrete excitations [2] as well as ionisation processes [3, 4, 5] for the two-electron system of hydrogen, the CCC method was extended to hydrogenic targets [6], and further to three-electron systems [7, 8, 9], such as for helium targets [10, 11, 12]. The CCC method was also extended to include double-photonionisation of helium-like targets [13, 14, 15].

While the CCC method yielded accurate total ionisation cross sections (TICS) for electron-impact ionisation on targets such as hydrogen and helium, the calculation of differential cross sections - namely the single-, double-, and triple-differential cross sections (SDCS, DDCS, TDCS) - were seen to fail to demonstrate convergence, discussed in detail by Bray [4]. That the scattering amplitudes calculated using the CCC method would lead to a good level of agreement with experimental values for the total ionisation cross sections, despite the non-convergence of the differential cross sections, proved quite puzzling. It was demonstrated by Bray [4], in the context of the Temkin-Poet model (also known as the S-wave model) [16, 17] of electron-impact hydrogen ionisation, that the SDCS is expected to be zero past the point of equal-energy-sharing between the projectile and ionised electrons. However, issues arise for the singlet case as the SDCS assumes a non-zero value at the point of equal-energy-sharing, leading to a discontinuity. These issues are compounded by the CCC method being restricted to evaluating ionisation amplitudes only for a countable number of outgoing projectile energies.

It was later shown by Stelbovics [5], that the behaviour of the singlet SDCS about the equal-energy-sharing point was indeed analogous to that of a Fourier series of a step function about the point of discontinuity. Specifically: that the singlet SDCS would not necessarily be zero past the point of equal-energy-sharing but would tend to zero, that the ionisation amplitudes would converge to half the step height at the equal-energy-sharing point, and thus that the SDCS would converge to one quarter the step height at this point. Accounting for this behaviour, Bray [9], was then able to demonstrate the validity of the CCC method by reproducing differential cross sections for electron-impact hydrogen ionisation which were in agreement with experimental results, as well as with the results of another computational approach: exterior complex scaling (ECS) [18].

The CCC method, having been proven capable of modelling elastic scattering and discrete excitations [2] as well as ionisation processes [3, 4, 5] for electron scattering on hydrogen, was extended to helium by Fursa and Bray [10, 11, 12].

It was demonstrated by Fursa and Bray [12] that the CCC method yielded accurate cross sections for elastic scattering and discrete excitations of the ground state of helium, 2^1S_0, with a frozen core model. However, it was observed that the cross sections for the metastable state 2^3S_1 did not produce acceptable agreement with experimental values and other computational values found in the literature. A later investigation by Bray and Fursa [19], incorporating the insights gained from the analysis of electron-impact ionisation of hydrogen, suggested that the CCC method yielded accurate ionisation amplitudes and differential cross sections for electron-impact ionisation of helium without excitation. Further investigation by Plottke *et al.* [20] into electron-impact excitation of helium indicated that the convergence of the auto-ionising doubly-excited discrete states was more involved than for the singly-excited states. However, convergence was demonstrated for these autoionising

states.

Notably, the Propagating Exterior Complex Scaling (PECS) method was applied by Bartlett and Stelbovics [21, 22], in the context of the S-wave model, to yield comprehensive total and differential cross sections for double ionisation, ionisation with excitation, and double excitation for helium. Agreement between the PECS and CCC methods was found for the total ionisation cross section without excitation, but not with excitation. Furthermore, an acceptable level of agreement between the methods was not found for the double excitation cross sections.

In summary, the CCC method is demonstrated to suitably model electron-impact collisions with helium in the ground state 2^1S_0, including elastic scattering, single-excitation and single-ionisation scattering processes. However, further development is required to calculate ionisation-with-excitation and double excitation cross sections which are in agreement with PECS calculations, and to calculate cross sections which are in agreement with experimental values for the metastable state 2^3S_1 of helium. We are primarily concerned with calculating total cross sections for electron-impact ionisation-with-excitation of ground state 2^1S_0 helium, which are in agreement with PECS calculations [22].

2 Theory

We shall present a brief derivation of the Convergent Close-Coupling (CCC) method for generalised electron-projectile atomic/ionic-target scattering, similar in form to the derivations presented in [8, 23]. We shall focus on the treatment of target ionisation, both with and without excitation, by consideration of the ionisation amplitudes within the CCC method.

2.1 Convergent Close-Coupling Method for an Atomic Target

In brief, the CCC method utilises the method of basis expansion to numerically solve the Lippmann-Schwinger equation in a momentum-space representation, for a projectile-target system, to yield the transition amplitudes, which are checked for convergence as the size of the basis is increased. The scattering statistics can then be extracted from the transistion amplitudes.

The rate of convergence, depends on many factors, such as the complexity of the target structure, the coupling between transition channels, and the choice of basis used in the expansion. With the selection of an appropriate basis, the unbounded continuum waves can be represented (to a sufficient accuracy) by a finite number of basis states, which allows ionisation amplitudes to be treated in a similar manner to discrete excitation amplitudes within the CCC method. A Laguerre basis is well-suited to this task; the benefits of this basis are discussed in further detail in [8, 5-9].

2.1.1 Laguerre Basis

To describe the target structure, the CCC method utilises a Laguerre basis $\{|\varphi_i\rangle\}_{i=1}^{\infty}$ for the Hilbert space $L^2(\mathbb{R}^3)$, for which the coordinate-space representation is of the form

$$\langle \mathbf{r}|\varphi_i\rangle = \varphi_i(r,\Omega) = \tfrac{1}{r}\xi_{k_i,li}(r)Y_{l_i}^{m_i}(\Omega), \tag{1}$$

where $Y_{l_i}^{m_i}(\Omega)$ are the spherical harmonics, and where $\xi_{k_i,l_i}(r)$ are the Laguerre radial basis functions, which are of the form

$$\xi_{k,l}(r) = \sqrt{\frac{\lambda_l(k-1)!}{(2l+1+k)!}}(\lambda_l r)^{l+1}\exp\!\left(-\tfrac{1}{2}\lambda_l r\right)L_{k-1}^{2l+2}(\lambda_l r), \tag{2}$$

where λ_l is the exponential fall-off, for each l, and where $L_{k-1}^{2l+2}(\lambda_l r)$ are the associated Laguerre polynomials. Note that we must have that $k_i \in \{1,2,\ldots\}$, $l_i \in \{0,1,\ldots\}$ and $m_i \in \{-\ell_i,\ldots,\ell_i\}$, for each $i \in \{1,2,\ldots\}$.

This Laguerre basis is utilised due to: the Laguerre basis functions $\{\varphi_i(r,\Omega)\}_{i=1}^{\infty}$ forming a complete basis for the Hilbert space $L^2(\mathbb{R}^3)$, the short-range and long-range behaviour of the radial basis functions being well suited to describing bound target states and providing a basis for expanding continuum states in, and because it allows the matrix representation of numerous operators to be calculated analytically.

Practically, we cannot utilise a basis of infinite size. Hence, we truncate the Laguerre radial basis $\{\xi_{k,l}(r)\}_{k=1}^{N_l}$ to a certain number of radial basis functions N_l, for each l, and we also truncate $l \in \{0,\ldots,l_{\max}\}$, limiting the maximum angular momentum we consider in our basis. Hence, for a given value of m, we have a basis size of

$$N = \sum_{l=0}^{l_{\max}} N_l. \tag{3}$$

In the limit as $N \to \infty$, the truncated basis will tend towards completeness, and it is in this limit that we discuss the convergence of the Convergent Close-Coupling method. We have presented the Laguerre basis with full generality, however we note that in the S-wave model we have $l_{\max} = 0$, which allows for the simplification of numerous expressions and computations.

2.1.2 Target States

Possessing now a suitable basis to work with, we proceed to represent the target in this basis by the method of basis expansion. Firstly, we note that electrons are indistinguishable fermionic particles; that is, no two electrons can be distinguished from each other, and they must satisfy Pauli's exclusion principle - that an electron state cannot be occupied by more than one electron. Since electrons are indistinguishable, we might naively suppose that the space of states consisting of n electrons is simply the n-th tensor power of the one-electron space, $T^n(\mathcal{H})$, defined by

$$T^n(\mathcal{H}) = \{|\psi_1\rangle \otimes \cdots \otimes |\psi_n\rangle : |\psi_1\rangle, \ldots, |\psi_n\rangle \in \mathcal{H}\}, \tag{4}$$

where $\mathcal{H}$ is the space of one-electron states. However this fails to account for Pauli's exclusion principle, since any one-electron state may be occupied up to n times. Hence, the space of states consisting of n electrons is instead defined to be the quotient space $\Lambda^n(\mathcal{H})$ of $T^n(\mathcal{H})$ by $\mathcal{D}^n$,

$$\Lambda^n(\mathcal{H}) = T^n(\mathcal{H})/\mathcal{D}^n, \tag{5}$$

where $\mathcal{D}^n \subset T^n(\mathcal{H})$ is the subspace of tensor products which contain any one-electron state more than once. The space $\Lambda^n(\mathcal{H})$ is known as the n-th exterior power of $\mathcal{H}$, and is identifiable as the subspace of $T^n(\mathcal{H})$ consisting of anti-symmetric tensors. Note that we shall adopt the following notation for tensor products

$$|\psi_1, \ldots, \psi_n\rangle = |\psi_1\rangle \otimes \cdots \otimes |\psi_n\rangle \tag{6}$$

and the following notation for anti-symmetric tensor products

$$|[\psi_1, \ldots, \psi_n]\rangle = \left|\psi_{[1,\ldots,n]}\right\rangle = \sqrt{n!}\hat{A}\,|\psi_1, \ldots, \psi_n\rangle \tag{7}$$

where $\hat{A} : T^n(\mathcal{H}) \to \Lambda^n(\mathcal{H})$ is the anti-symmetriser operator which we define to be of the form

$$\hat{A}\,|\psi_1, \ldots, \psi_n\rangle = \frac{1}{n!} \sum_{\sigma \in S_n} \mathrm{sgn}(\sigma) \left|\psi_{\sigma(1)}, \ldots, \psi_{\sigma(n)}\right\rangle, \tag{8}$$

where S_n is the symmetric group on n elements, the sum is taken over all permutations $\sigma \in S_n$, and where $\mathrm{sgn}(\sigma)$ is the signature of the permutation σ. It follows from this construction that

$$\left|\psi_{[a_1,\ldots,a_n]}\right\rangle = 0 \quad \text{if any} \quad a_i = a_j, \tag{9}$$

hence satisfying Pauli's exclusion principle. Furthermore, we have that

$$\hat{P}_{i,j} \left|\psi_{[1,\ldots,n]}\right\rangle = -\left|\psi_{[1,\ldots,n]}\right\rangle, \tag{10}$$

where $\hat{P}_{i,j}$ is the pairwise exchange operator, permuting the states $|\psi_i\rangle$ and $|\psi_j\rangle$. We note that in this context, the states $|\psi_i\rangle$ include both coordinate and spin states.

It follows that for an atomic/ionic target, consisting of n_e electrons, the space of target states is of the form $\mathcal{H}_T = \Lambda^{n_\mathrm{e}}(\mathcal{H})$. We shall adopt the convention that operators which act on the m-th electron space (including the projectile electron), will be indexed by m, for $m = 0, 1, \ldots, n_\mathrm{e}$, with $m = 0$ indexing the projectile electron space.

Target Hamiltonian The target Hamiltonian, for an atomic/ionic target with n_e electrons, is of the form

$$\hat{H}_T = \sum_{m=1}^{n_\mathrm{e}} \hat{K}_m + \sum_{m=1}^{n_\mathrm{e}} \hat{V}_m + \sum_{m=1}^{n_\mathrm{e}} \sum_{n=m+1}^{n_\mathrm{e}} \hat{V}_{m,n}, \tag{11}$$

where $\hat{K}_m$ and $\hat{V}_m$ are the target electron kinetic and electron-nuclei potential operators, for $m = 1, \ldots, n_\mathrm{e}$, and where $\hat{V}_{m,n}$ are the electron-electron potential operators, for $m, n = 1, \ldots, n_\mathrm{e}$.

Target Diagonalisation The target Hamiltonian, restricted to just one target electron,

$$\hat{H}_{T,\mathrm{e}} = \hat{K}_1 + \hat{V}_1, \tag{12}$$

is expanded in a Laguerre basis $\{|\varphi_i\rangle\}_{i=1}^N$ and diagonalised to yield a set of one-electron atomic orbitals $\{\,|\phi_i^{(N)}\rangle\}_{i=1}^N$ which are orthonormal and satisfy

$$\langle\phi_i^{(N)}|\,\hat{H}_{T,\mathrm{e}}\,|\phi_j^{(N)}\rangle = \varepsilon_i^{(N)}\delta_{i,j}. \tag{13}$$

From these one-electron atomic orbitals, we generate a set of one-electron spin orbitals $\{\,|\chi_i^{(N)}\rangle\}_{i=1}^{2N}$ for which $|\chi_{2i-1}^{(N)}\rangle$ and $|\chi_{2i}^{(N)}\rangle$ both correspond to $|\phi_i^{(N)}\rangle$ but have spin projection $\frac{1}{2}$ and $-\frac{1}{2}$ respectively. These one-electron spin orbitals are then combined to construct Slater determinants; for any selection of n_e one-electron spin orbitals $|\chi_{a_1}^{(N)}\rangle, \ldots, |\chi_{a_{n_\mathrm{e}}}^{(N)}\rangle \in \{\,|\chi_i^{(N)}\rangle\}_{i=1}^{2N}$, the Slater determinant of these spin orbitals is of the form

$$|\chi_{[a_1,\ldots,a_{n_\mathrm{e}}]}^{(N)}\rangle = \sqrt{n_\mathrm{e}!}\hat{A}\,|\chi_{a_1}^{(N)},\ldots,\chi_{a_{n_\mathrm{e}}}^{(N)}\rangle = \frac{1}{\sqrt{n_\mathrm{e}!}}\sum_{\sigma\in S_{n_\mathrm{e}}}\mathrm{sgn}(\sigma)\,|\chi_{a_{\sigma(1)}}^{(N)},\ldots,\chi_{a_{\sigma(n_\mathrm{e})}}^{(N)}\rangle\,, \tag{14}$$

as per (7) and (8). We note that Slater determinants are anti-symmetric under pairwise exchange of any two orbitals, and are zero if constructed with two spin orbitals in the same state. Hence they adhere to Pauli's exclusion principle and are indeed elements of $\mathcal{H}_T = \Lambda^{n_\mathrm{e}}(\mathcal{H})$.

The true target states $\{|\Phi_\alpha\rangle\} \in \mathcal{H}_T$ are then approximated by expanding the full target Hamiltonian $\hat{H}_T$ in a basis of Slater determinants,

$$\big\{\,|\chi_{[a_1,\ldots,a_{n_\mathrm{e}}]}^{(N)}\rangle : a_1,\ldots,a_{n_\mathrm{e}} \in \{1,\ldots,2N\}\big\}, \tag{15}$$

and diagonalising to yield a set of target pseudostates $\{\,|\Phi_n^{(N)}\rangle\}_{n=1}^{N_T}$ which are orthonormal and satisfy

$$\langle\Phi_i^{(N)}|\,\hat{H}_T\,|\Phi_j^{(N)}\rangle = \epsilon_i^{(N)}\delta_{i,j}, \tag{16}$$

where $\epsilon_n^{(N)}$ is the pseudoenergy corresponding to the pseudostate $|\Phi_n^{(N)}\rangle$. Note that the number of target pseudostates N_T depends on the number of Slater determinants utilised in the expansion of $\hat{H}_T$. Note also that the (N) superscript has been introduced to indicate that these are not true eigenstates of the target Hamiltonian, only of its representation in the truncated Laguerrre basis, and that these pseudostates and their pseudoenergies are dependent on the size of the Laguerre basis utilised.

We remark that the target pseudostates will be expressed as a linear combination of Slater determinants of the form

$$|\Phi_n^{(N)}\rangle = \sum_{1\le a_1<\ldots<a_{n_\mathrm{e}}\le 2N} D_n^{a_1,\ldots,a_{n_\mathrm{e}}}\,|\chi_{[a_1,\ldots,a_{n_\mathrm{e}}]}^{(N)}\rangle \tag{17}$$

where $D_n^{a_1,\ldots,a_{n_e}}$ are the expansion coefficients. The summation indices are taken over only linearly independent Slater determinants; a consequence of the anti-symmetry of the Slater determinants under pairwise exchange of any two orbitals. In this context, the Slater determinants are often referred to as (electron) configurations, being the assembly of n_e one-electron configurations.

Using all possible Slater determinants in the expansion is often computationally infeasible, as the number of determinants scales as $\binom{2N}{n_e}$. A common method of mitigating this computational hindrance, which we shall utilise, is to use only a subset of the full set of Slater determinants, for which the span of this subset remains sufficiently able to describe the target pseudostates to a required degree of accuracy. Specifically, the target orbitals are partitioned into a core set and valence set of orbitals, with the core orbitals being limited to a much smaller set of states, while the valence orbitals are not so constrained. This provides an effective model for targets with a mostly fixed set of core electron states, while allowing the valence electrons to interact fully with the projectile.

Completeness of Target Pseudostates As a result of the completeness of the Laguerre basis, the set of target pseudostates will be separable into a set of bounded pseudostates which will form an approximation of the true target discrete spectrum, and a set of unbounded pseudostates which will provide a discretisation of the true continuum of unbounded states. Without loss of generality, we order the target pseudostates by increasing pseudoenergy, $\epsilon_1^{(N)} < \ldots < \epsilon_{N_T}^{(N)}$, which allows us to express the separability of the spectrum in the form

$$\{\,|\Phi_n^{(N)}\rangle\}_{n=1}^{N_T} = \{\,|\Phi_n^{(N)}\rangle\}_{n=1}^{N_B} \cup \{\,|\Phi_n^{(N)}\rangle\}_{n=N_B+1}^{N_T}, \tag{18}$$

where $\epsilon_n^{(N)} < 0$ for $n = 1, \ldots, N_B$, and where $\epsilon_n^{(N)} \geq 0$ for $n = N_B + 1, \ldots, N_T$. Note that N_B is the number of bounded pseudostates, and we write $N_U = N_T - N_B$ to represent the number of unbounded pseudostates, both of which are dependent on N by consequence of the construction of the target pseudostates.

The projection operator for the target pseudostates, $\hat{I}_T^{(N)}$, is of the form

$$\hat{I}_T^{(N)} = \sum_{n=1}^{N_T} |\Phi_n^{(N)}\rangle\langle\Phi_n^{(N)}| = \sum_{n=1}^{N_B} |\Phi_n^{(N)}\rangle\langle\Phi_n^{(N)}| + \sum_{n=N_B+1}^{N_T} |\Phi_n^{(N)}\rangle\langle\Phi_n^{(N)}|\,, \tag{19}$$

and so in the limit as $N \to \infty$, the sum over the bounded pseudostates will converge to the sum over the true target discrete states and the sum over the unbounded pseudostates will converge to a discretisation of the integral over the true continuum spectrum. Whence, it follows that projection operator for the target pseudostates converges to the identity operator, for $\mathcal{H}_T$, in the limit as $N \to \infty$; that is,

$$\lim_{N\to\infty} \hat{I}_T^{(N)} = \hat{I}_T. \tag{20}$$

A more rigorous discussion on the suitabiliy of representing unbounded states in the Laguerre basis is provided in [8, 5-9].

2.1.3 Total Wavefunction

The total wavefunction $|\Psi^{(+)}\rangle \in \Lambda^{1+n_e}(\mathcal{H})$ is defined to be an eigenstate of the total Hamiltonian $\hat{H}$ with total energy E and specified to have outgoing spherical-wave boundary conditions,

$$\hat{H}\,|\Psi^{(+)}\rangle = E\,|\Psi^{(+)}\rangle\,, \tag{21}$$

where $\hat{H}$ is of the form

$$\hat{H} = \hat{H}_T + \hat{K}_0 + \hat{V}_0 + \sum_{m=1}^{n_e} \hat{V}_{0,m}, \tag{22}$$

where $\hat{H}_T$ is the target Hamiltonian, defined in (11), $\hat{K}_0$ is the projectile electron kinetic operator, $\hat{V}_0$ is the projectile electron-nuclei potential operator, and $\hat{V}_{0,m}$ are the projectile electron-target electron potential operators. The following treatment of the total wavefunction is of a similar form to [23, 202-204].

To ensure that the total wavefunction is anti-symmetric we utilise the anti-symmetriser, defined in (8), to construct it explicitly

$$|\Psi^{(+)}\rangle = \hat{A}\,|\psi^{(+)}\rangle = \left[1 - \sum_{m=1}^{n_e} \hat{P}_{0,m}\right] |\psi^{(+)}\rangle\,, \tag{23}$$

where $\hat{P}_{0,m}$ are the pairwise electron exchange operators defined in (10), and where $|\psi^{(+)}\rangle \in \mathcal{H}_T \otimes \mathcal{H}$ is the unsymmetrised total wavefunction. As the target states are already anti-symmetric by construction, the anti-symmetriser has assumed a simpler form - requiring only permutations of the unsymmetrised projectile state with the spin-orbital states of the target electrons. Note that we have omitted the $(1 + n_e)!$ term in $\hat{A}$, since it is a scalar term which can be normalised away when required.

To construct the unsymmetrised total wavefunction $|\psi^{(+)}\rangle$ we perform a multichannel expansion, projecting it onto the target psuedostates,

$$|\psi^{(N,+)}\rangle = \hat{I}_T^{(N)}\,|\psi^{(+)}\rangle = \sum_{n=1}^{N_T} |\Phi_n^{(N)}\rangle\,\langle\Phi_n^{(N)}|\psi^{(+)}\rangle = \sum_{n=1}^{N_T} |\Phi_n^{(N)} F_n^{(N)}\rangle\,, \tag{24}$$

where $|F_n^{(N)}\rangle = \langle\Phi_n^{(N)}|\psi^{(+)}\rangle$ are the multichannel weight functions, and note that as a result of (20), that

$$|\psi^{(+)}\rangle = \lim_{N\to\infty} \hat{I}_T^{(N)}\,|\psi^{(+)}\rangle = \lim_{N\to\infty} |\psi^{(N,+)}\rangle\,. \tag{25}$$

Similarly, the total wavefunction constructed from the projection of the unsymmetrised total wavefunction onto the target pseudostates is written in the form

$$|\Psi^{(N,+)}\rangle = \hat{A}\,|\psi^{(N,+)}\rangle = \left[1 - \sum_{m=1}^{n_e} \hat{P}_{0,m}\right] |\psi^{(N,+)}\rangle\,, \tag{26}$$

and we note that as a result of (20), that

$$|\Psi^{(+)}\rangle = \lim_{N\to\infty} |\Psi^{(N,+)}\rangle\,. \tag{27}$$

However, after projecting the unsymmetrised total wavefunction with the projection operator for the target pseudostates, the multichannel expansion is not uniquely defined, since for any state $|\omega^{(N)}\rangle \in \ker(\hat{A}\hat{I}_T^{(N)})$ and scalar $\alpha \in \mathbb{C}$, the multichannel expansion of $|\psi^{(N,+)}\rangle + \alpha\,|\omega^{(N)}\rangle$ will be identical to that of $|\psi^{(N,+)}\rangle$. To resolve this dilemma, we first note that the multichannel weight functions $|F_n^{(N)}\rangle$ are within the span of the one-electron spin orbitals $\{\,|\chi_i^{(N)}\rangle\}_{i=1}^{2N}$, used to construct

the Slater determinants, (14), with which the target states are expanded. Hence, we impose the constraint that for any of the one-electron spin orbitals $|\chi_i^{(N)}\rangle$, that

$$\hat{P}_{0,m} |\Phi_n^{(N)} \chi_i^{(N)}\rangle = - |\Phi_n^{(N)} \chi_i^{(N)}\rangle \,. \tag{28}$$

which can be seen as an explicit imposition of (10). With this constraint in place, it can then be shown that $\dim \ker(\hat{A}\hat{I}_T^{(N)}) = 0$, whence it follows that the multichannel expansion of $|\psi^{(N,+)}\rangle$ is now unique in determining $|\Psi^{(N,+)}\rangle$.

2.1.4 Convergent Close-Coupling Equations

We present a derivation for the Convergent Close-Coupling (CCC) equations, beginning with the Schrödinger equation for the total wavefunction $|\Psi^{(+)}\rangle$ presented in (21). This shall be re-arranged to yield the Lippmann-Schwinger equation, which will then be solved using the CCC formalism to obtain the matrix elements of the $\hat{T}$ operator - with which scattering statistics can be calculated.

Lippmann-Schwinger Equation We consider an eigenstate $|\Psi\rangle$ of a Hamiltonian $\hat{H}$, with eigenenergy E, for which the Schrödinger equation is of the form

$$\hat{H} |\Psi\rangle = \hat{H}_\mathrm{A} |\Psi\rangle + \hat{V} |\Psi\rangle = E |\Psi\rangle \,, \tag{29}$$

where $\hat{H}_\mathrm{A}$ is the unbounded asymptotic Hamiltonian and $\hat{V}$ is a potential. This expression can be rearranged to the form

$$[E - \hat{H}_\mathrm{A}] |\Psi\rangle = \hat{V} |\Psi\rangle \,. \tag{30}$$

Suppose that $\{ |\Omega_\alpha\rangle \}$ are the (countably and uncountably infinite) eigenstates of the asymptotic Hamiltonian, with corresponding eigenvalues ε_α,

$$\hat{H}_\mathrm{A} |\Omega_\alpha\rangle = \varepsilon_\alpha |\Omega_\alpha\rangle \,. \tag{31}$$

We note that where $\varepsilon_\alpha = E$, it follows that $|\Omega_\alpha\rangle \in \ker(E - \hat{H}_\mathrm{A})$; for a given energy E, we denote these particular asymptotic states by $|\Omega_\alpha^{(E)}\rangle$ and say that they are on-shell states, and that the energies of these states are on-shell. We now define the Green's operator $\hat{G}_{(E)}$, to be such that

$$\hat{G}_{(E)}[E - \hat{H}_\mathrm{A}] = \hat{I} = [E - \hat{H}_\mathrm{A}]\hat{G}_{(E)}, \tag{32}$$

whence we obtain a general form of the Lippmann-Schwinger equation,

$$|\Psi\rangle = \sum_{\alpha:\varepsilon_\alpha = E} \int C_\alpha |\Omega_\alpha^{(E)}\rangle + \hat{G}_{(E)} \hat{V} |\Psi\rangle \,, \tag{33}$$

where C_α are arbitrary scalar coefficients. We note that in this context, the sum taken over the indexes of the asymptotic eigenstates represents a sum over the countably infinite states, and an integration over the uncountably infinite states, for which the eigenenergy ε_α is equal to E. The inclusion of the selected asymptotic eigenstates is required as they are in the kernel of $[E - \hat{H}_\mathrm{A}]$, thus forming the homogenous solutions to the Lippmann-Schwinger equation. This can be demonstrated

by applying the operator $[E - \hat{H}_{\mathrm{A}}]$ on the left of (33),

$$\begin{aligned}[E - \hat{H}_{\mathrm{A}}]\,|\Psi\rangle &= \sum_{\alpha:\varepsilon_\alpha = E} \int C_\alpha [E - \hat{H}_{\mathrm{A}}]\,|\Omega_\alpha^{(E)}\rangle + [E - \hat{H}_{\mathrm{A}}]\hat{G}_{(E)}\hat{V}\,|\Psi\rangle \\ &= \sum_{\alpha:\varepsilon_\alpha = E} \int C_\alpha\,|0\rangle + \hat{I}\hat{V}\,|\Psi\rangle \\ &= \hat{V}\,|\Psi\rangle\,.\end{aligned}$$

At this point, we note that selecting the values of the coefficients C_α amounts to specifying a boundary condition for the eigenstate $|\Psi\rangle$. By consequence of the linearity of (33), we may therefore simplify the generalised sum/integral, without loss of generality, by considering eigenstates of the form

$$|\Psi_\alpha\rangle = |\Omega_\alpha^{(E)}\rangle + \hat{G}_{(E)}\hat{V}\,|\Psi_\alpha\rangle\,, \tag{34}$$

for a particular $|\Omega_\alpha^{(E)}\rangle \in \ker(E - \hat{H}_{\mathrm{A}})$, and we say that $|\Psi_\alpha\rangle$ is the eigenstate of $\hat{H}$ corresponding to the boundary condition specified by the asymptotic eigenstate $|\Omega_\alpha^{(E)}\rangle$. We now define the $\hat{T}$ operator to be such that

$$|\Psi_\alpha\rangle = [\hat{I} + \hat{G}_{(E)}\hat{T}]\,|\Omega_\alpha^{(E)}\rangle\,, \tag{35}$$

which is equivalently defined by writing

$$\hat{T}\,|\Omega_\alpha^{(E)}\rangle = \hat{V}\,|\Psi_\alpha\rangle\,. \tag{36}$$

Furthermore, we have that

$$\begin{aligned}|\Psi_\alpha\rangle &= |\Omega_\alpha^{(E)}\rangle + \hat{G}_{(E)}\hat{V}\,|\Psi_\alpha\rangle \\ &= |\Omega_\alpha^{(E)}\rangle + \hat{G}_{(E)}\hat{V}\big[\hat{I} + \hat{G}_{(E)}\hat{T}\big]\,|\Omega_\alpha^{(E)}\rangle \\ &= \big[\hat{I} + \hat{G}_{(E)}\hat{V} + \hat{G}_{(E)}\hat{V}\hat{G}_{(E)}\hat{T}\big]\,|\Omega_\alpha^{(E)}\rangle \\ &= \big[\hat{I} + \hat{G}_{(E)}(\hat{V} + \hat{V}\hat{G}_{(E)}\hat{T})\big]\,|\Omega_\alpha^{(E)}\rangle\,,\end{aligned}$$

whence it follows that $\hat{T}$ can be written in the form

$$\hat{T}\,|\Omega_\alpha^{(E)}\rangle = [\hat{V} + \hat{V}\hat{G}_{(E)}\hat{T}]\,|\Omega_\alpha^{(E)}\rangle\,, \tag{37}$$

yielding the formulation of the Lippmann-Schwinger equation in terms of the $\hat{T}$ operator. At this point we consider the explicit form of the Green's operator $\hat{G}_{(E)}$. First, we note that the asymptotic eigenstates are complete in the sense that they provide a resolution of the identity

$$\hat{I} = \sum_\gamma \int |\Omega_\gamma\rangle\langle\Omega_\gamma|\,, \tag{38}$$

and a spectral decomposition of the asymptotic Hamiltonian

$$\hat{H}_{\mathrm{A}} = \sum_\gamma \int \varepsilon_\gamma\,|\Omega_\gamma\rangle\langle\Omega_\gamma|\,.$$

It therefore follows from the definition of the Green's operator, (32), that we must have

$$\hat{G}_{(E)}[E - \hat{H}_{\mathrm{A}}] = \hat{I}$$
$$\sum_{\gamma} \int (E - \varepsilon_{\gamma}) \hat{G}_{(E)} \left|\Omega_{\gamma}\right\rangle\!\left\langle\Omega_{\gamma}\right| = \sum_{\gamma} \int \left|\Omega_{\gamma}\right\rangle\!\left\langle\Omega_{\gamma}\right|,$$

whence it follows that the spectral decomposition of the Green's operator is of the form

$$\hat{G}_{(E)} = \sum_{\gamma} \int \frac{\left|\Omega_{\gamma}\right\rangle\!\left\langle\Omega_{\gamma}\right|}{E - \varepsilon_{\gamma}}. \tag{39}$$

However, this expression is not well-defined, as it is singular for the asymptotic states $|\Omega_{\gamma}^{(E)}\rangle$ for which $\varepsilon_{\gamma} = E$. This problem can be overcome by regularising the Green's operator to either the incoming $\hat{G}_{(E,-)}$ or outgoing $\hat{G}_{(E,+)}$ forms,

$$\hat{G}_{(E,\pm)} = \lim_{\eta \to 0} \sum_{\gamma} \int \frac{\left|\Omega_{\gamma}\right\rangle\!\left\langle\Omega_{\gamma}\right|}{E - \varepsilon_{\gamma} \pm \mathrm{i}\eta} = \sum_{\gamma} \int \frac{\left|\Omega_{\gamma}\right\rangle\!\left\langle\Omega_{\gamma}\right|}{E - \varepsilon_{\gamma} \pm \mathrm{i}0}, \tag{40}$$

where the presence of the imaginary limit ensures that the integral is well-defined for all ε_{γ}. We elect to use the outgoing Green's operator $\hat{G}_{(E,+)}$ as we are concerned with the outgoing behaviour of the eigenstate $|\Psi_{\alpha}^{(+)}\rangle$. We can now re-write the Lippmann-Schwinger equation in the following form

$$\langle\Omega_{\alpha}|\hat{T}|\Omega_{\beta}^{(E)}\rangle = \langle\Omega_{\alpha}|\hat{V}|\Omega_{\beta}^{(E)}\rangle + \sum_{\gamma} \int \frac{\langle\Omega_{\alpha}|\hat{V}|\Omega_{\gamma}\rangle \, \langle\Omega_{\gamma}|\hat{T}|\Omega_{\beta}^{(E)}\rangle}{E - \varepsilon_{\gamma} + \mathrm{i}0}, \tag{41}$$

which expresses the representation of the operator $\hat{T}$, for a given energy E, in terms of the asymptotic eigenstates $\{\,|\Omega_{\alpha}\rangle\}$ and the on-shell asymptotic eigenstates $\{\,|\Omega_{\beta}^{(E)}\rangle\}$.

Convergent Close-Coupling Formalism In the Convergent Close-Coupling formalism, the Lippmann-Schwinger equation in terms of the $\hat{T}$ operator, (41), is solved in momentum space. We preface this discussion with a minor note, that the notation for the asymptotic Hamiltonian $\hat{H}_{\mathrm{A}}$ is to be distinguished from the notation for the anti-symmetriser $\hat{A}$, and is unrelated.

We split the Hamiltonian, from (22), into an asymptotic Hamiltonian and a potential in the form

$$\hat{H} = \hat{H}_T + \hat{K}_0 + \hat{V}_0 + \sum_{m=1}^{n_{\mathrm{e}}} \hat{V}_{0,m} = \hat{H}_{\mathrm{A}} + \hat{W}, \tag{42}$$

where the asymptotic Hamiltonian is of the form

$$\hat{H}_{\mathrm{A}} = \hat{H}_T + \hat{K}_0 + \hat{U}_0, \tag{43}$$

and where the potential, modelling the interaction between the projectile and target states, is of the form

$$\hat{W} = \hat{V}_0 + \sum_{m=1}^{n_{\mathrm{e}}} \hat{V}_{0,m} - \hat{U}_0, \tag{44}$$

where $\hat{U}_0$ is an asymptotic potential acting on the projectile, which can be chosen arbitrarily. A suitable choice for this potential is that of a Coulomb potential with a charge corresponding to the asymptotic charge of the target system, whence $\langle \mathbf{r}|\hat{W}\rangle = W(r,\Omega) \to 0$ as $r \to \infty$. Such a selection for $\hat{U}_0$ adapts the projectile states to the target system, without loss of generality, and can lead to improvement in computational performance, as discussed in [23, 204].

The asymptotic eigenstates are therefore taken to be of the form

$$|\Omega_\alpha\rangle = |\Phi_\alpha \mathbf{k}_\alpha\rangle \approx |\Phi^{(N)}_{n_\alpha}\mathbf{k}_\alpha\rangle\,, \tag{45}$$

where $\{|\Phi^{(N)}_n\rangle\}_{i=1}^{N_T}$ are the target pseudostates, defined in (16), which satisfy

$$\langle\Phi^{(N)}_i|\hat{H}_T|\Phi^{(N)}_j\rangle = \epsilon^{(N)}_i \delta_{i,j}, \tag{46}$$

and where $|\mathbf{k}_\alpha\rangle$ are the continuum waves (which could be plane, distorted, or Coulomb waves depending on the choice of $\hat{U}_0$), defined to be eigenstates of the projectile component of the asymptotic Hamiltonian,

$$[\hat{K}_0 + \hat{U}_0]\,|\mathbf{k}_\alpha\rangle = \tfrac{1}{2}k^2_\alpha\,|\mathbf{k}_\alpha\rangle\,, \tag{47}$$

whence it can be seen that the asymptotic eigenenergies are of the form

$$\varepsilon_\alpha = \epsilon_{n_\alpha} + \tfrac{1}{2}k^2_\alpha \approx \epsilon^{(N)}_{n_\alpha} + \tfrac{1}{2}k^2_\alpha. \tag{48}$$

Furthermore, the total wavefunction is taken to be of the form

$$|\Psi^{(+)}_\alpha\rangle = \hat{A}\,|\psi^{(+)}_\alpha\rangle \approx \hat{A}\hat{I}^{(N)}_T\,|\psi^{(+)}_\alpha\rangle = \hat{A}\,|\psi^{(N,+)}_\alpha\rangle = |\Psi^{(N,+)}_\alpha\rangle\,, \tag{49}$$

as in (23), where $\hat{A}$ is the anti-symmetriser operator, defined in (8), and is subject to the constraints imposed in (28) to ensure uniqueness. We note that with these expressions for the asymptotic eigenstates and the total wavefunction, that the $\hat{T}$ operator is related to the potential $\hat{W}$ by the expression

$$\hat{T}\,|\Phi^{(N)}_{n_\alpha}\mathbf{k}_\alpha\rangle = \hat{W}\,|\Psi^{(N,+)}_\alpha\rangle = \hat{W}\hat{A}\hat{I}^{(N)}_T\,|\psi^{(+)}_\alpha\rangle = \hat{W}\hat{A}\,|\psi^{(N,+)}_\alpha\rangle\,. \tag{50}$$

However, it is possible to recast the potential $\hat{W}$ in a form $\hat{V}$ which accounts for the explicit anti-symmetrisation of the total wavefunction; that is, which allows us to write the CCC equations without direct reference to the anti-symmetriser $\hat{A}$. To do this, we first note that

$$0 = [E - \hat{H}]\,|\Psi^{(+)}_\alpha\rangle = [E - \hat{H}]\hat{A}\,|\psi^{(+)}_\alpha\rangle\,,$$

with the operator on the right hand side expanding to the form

$$[E - \hat{H}]\hat{A} = \left[E - \hat{H} - [E - \hat{H}]\sum_{m=1}^{n_\mathrm{e}}\hat{P}_{0,m}\right] = \left[E - \hat{H}_\mathrm{A} - \hat{W} - [E - \hat{H}]\sum_{m=1}^{n_\mathrm{e}}\hat{P}_{0,m}\right],$$

where again we make sure to distinguish the notation for the asymptotic Hamiltonian $\hat{H}_\mathrm{A}$ and the anti-symmetriser $\hat{A}$. We therefore define the explicitly anti-symmetrised potential $\hat{V}$ to be of the form

$$\hat{V} = \hat{W} + [E - \hat{H}]\sum_{m=1}^{n_\mathrm{e}}\hat{P}_{0,m} = \hat{V}_0 + \sum_{m=1}^{n_\mathrm{e}}\hat{V}_{0,m} - \hat{U}_0 + [E - \hat{H}]\sum_{m=1}^{n_\mathrm{e}}\hat{P}_{0,m}, \tag{51}$$

for which we can see that

$$0 = [E - \hat{H}]\hat{A}\,|\psi_\alpha^{(+)}\rangle = [E - [\hat{H}_\mathrm{A} + \hat{V}]]\,|\psi_\alpha^{(+)}\rangle\,,$$

which is to say that the Lippmann-Schwinger equation (41) can be written in terms of the unsymmetrised total wavefunction $|\psi_\alpha^{(+)}\rangle$, rather than the anti-symmetric total wavefunction $|\Psi_\alpha^{(+)}\rangle$. Specifically, this allows us to write the $\hat{T}$ operator in the form

$$\hat{T}\,|\Phi_{n_\alpha}^{(N)}\mathbf{k}_\alpha\rangle = \hat{V}\hat{I}_T^{(N)}\,|\psi_\alpha^{(+)}\rangle = \hat{V}\,|\psi_\alpha^{(N,+)}\rangle\,. \tag{52}$$

We then have the Convergent Close-Coupling equations in terms of the $\hat{T}$ operator

$$\begin{aligned}\langle \mathbf{k}_f \Phi_{n_f}^{(N)}|\hat{T}|\Phi_{n_i}^{(N)}\mathbf{k}_i\rangle = {} & \langle \mathbf{k}_f \Phi_{n_f}^{(N)}|\hat{V}|\Phi_{n_i}^{(N)}\mathbf{k}_i\rangle \\ & + \sum_{n=1}^{N_T}\int \mathrm{d}\mathbf{k}\,\frac{\langle \mathbf{k}_f \Phi_{n_f}^{(N)}|\hat{V}|\Phi_n^{(N)}\mathbf{k}\rangle\ \langle \mathbf{k}\Phi_n^{(N)}|\hat{T}|\Phi_{n_i}^{(N)}\mathbf{k}_i\rangle}{E - \epsilon_n^{(N)} - \frac{1}{2}k^2 \pm \mathrm{i}0},\end{aligned} \tag{53}$$

forming a set of $\mathbb{C}$-valued matrix equations which are numerically solved to yield the T matrix, from which information about the total wavefunction $|\Psi_i^{(N,+)}\rangle$ can be derived. However, it is possible to re-write the Convergent Close-Coupling equations in terms of an operator $\hat{K}$,

$$\begin{aligned}\langle \mathbf{k}_f \Phi_{n_f}^{(N)}|\hat{K}|\Phi_{n_i}^{(N)}\mathbf{k}_i\rangle = {} & \langle \mathbf{k}_f \Phi_{n_f}^{(N)}|\hat{V}|\Phi_{n_i}^{(N)}\mathbf{k}_i\rangle \\ & + \sum_{n=1}^{N_T}\mathcal{P}\int \mathrm{d}\mathbf{k}\,\frac{\langle \mathbf{k}_f \Phi_{n_f}^{(N)}|\hat{V}|\Phi_n^{(N)}\mathbf{k}\rangle\ \langle \mathbf{k}\Phi_n^{(N)}|\hat{K}|\Phi_{n_i}^{(N)}\mathbf{k}_i\rangle}{E - \epsilon_n^{(N)} - \frac{1}{2}k^2},\end{aligned} \tag{54}$$

where $\mathcal{P}$ indicates that the principal value of the integral is taken, which forms a set of $\mathbb{R}$-valued matrix equations which can be solved more efficiently, to yield the K matrix. The T matrix can then be reconstructed from the K matrix by the identity [8, 9]

$$\langle \mathbf{k}_f \Phi_{n_f}^{(N)}|\hat{K}|\Phi_{n_i}^{(N)}\mathbf{k}_i\rangle = \sum_{n=1}^{N_T}\langle \mathbf{k}_f \Phi_{n_f}^{(N)}|\hat{T}|\Phi_n^{(N)}\mathbf{k}_n\rangle\left(\delta_{n,i} + \mathrm{i}\pi k_n\,\langle \mathbf{k}_n \Phi_n^{(N)}|\hat{K}|\Phi_{n_i}^{(N)}\mathbf{k}_i\rangle\right), \tag{55}$$

where k_n are the on-shell projectile momenta which satisfy

$$E = \epsilon_n^{(N)} + \tfrac{1}{2}k_n^2 \quad \text{for} \quad n = 1, \ldots, N_T. \tag{56}$$

We note that the matrix equations (53), as well as (54) and (55), are computationally parameterised by the set of target pseudostates $\{\,|\Phi_n^{(N)}\rangle\}_{n=1}^{N_T}$ and the discretisation of the projectile spectrum. In turn, the target pseudostates are parameterised by the number of Slater determinants N_T used in their construction, and the number of basis functions N used to construct the one-electron orbitals from which the Slater determinants are built. Furthermore, we note that matrix equations in this form do not explicitly include the constraints, detailed in (28), which guarantee the uniqueness of the explicitly anti-symmetrised multichannel expansion.

2.2 Scattering Statistics

At this point, we shall make explicit use of the S-wave model, wherein all partial wave expansions are limited to the $l = 0$ terms; this has the effect of restricting our attention to asymptotic eigenstates

$|\Phi_n^{(N)}\mathbf{k}\rangle$ for which the target pseudostate has $l = 0$. This allows for a simpler presentation of the theory, and a significant reduction in computational complexity. Furthermore, calculations performed in the S-wave model are sufficient for the emergence of scattering phenomena with which we are interested. Much of the following treatment is generalisable to the inclusion of arbitrary angular momentum.

Lastly, we note that many of the following statistics can be constructed for a particular symmetry of the system which is conserved by the scattering process; examples include total spin and angular momentum. We shall refrain from specifying the forms of these statistics for specific symmetries, in lieu of providing a clearer, more general treatment.

2.2.1 Scattering Amplitudes

Once calculated, the matrix elements of the $\hat{T}$ operator yield the transition amplitudes between asymptotic states, which can then be used to calculate the scattering amplitudes. In general terms, the scattering amplitudes can be written in the form

$$f_{\alpha,\beta} = f_{\alpha,\beta}(\mathbf{k}_\alpha, \mathbf{k}_\beta) = \langle \mathbf{k}_\alpha \Phi_\alpha | \hat{V} | \Psi_\beta \rangle = \langle \mathbf{k}_\alpha \Phi_\alpha | \hat{T} | \Phi_\beta \mathbf{k}_\beta \rangle \,, \tag{57}$$

where the target state $|\Phi_\alpha\rangle$ can be a bounded discrete state or an unbounded continuum state, corresponding to either an elastic scattering / a discrete excition transition, or an ionisation transition. For discrete excitations, the numerically calculated scattering amplitude is simply of the form

$$f_{f,i}^{(N)} = f_{n_f,n_i}^{(N)}(\mathbf{k}_f, \mathbf{k}_i) = \langle \mathbf{k}_f \Phi_{n_f}^{(N)} | \hat{T} | \Phi_{n_i}^{(N)} \mathbf{k}_i \rangle \,, \tag{58}$$

for on-shell transitions,

$$\epsilon_{n_f}^{(N)} + \tfrac{1}{2}k_f^2 = E = \epsilon_{n_i}^{(N)} + \tfrac{1}{2}k_i^2, \tag{59}$$

with elastic scattering occurring in the case where $n_f = n_i$,

$$f_i^{(N)}(\mathbf{k}_f, \mathbf{k}_i) = f_{n_i,n_i}^{(N)}(\mathbf{k}_f, \mathbf{k}_i) = \langle \mathbf{k}_f \Phi_{n_i}^{(N)} | \hat{T} | \Phi_{n_i}^{(N)} \mathbf{k}_i \rangle \,. \tag{60}$$

However, the numerically calculated scattering amplitudes for ionisations, hereby referred to as ionisation amplitudes, require a more carefully considered treatment - which we present in a form similar to that described in [9, 24]. We shall restrict our attention to the case of single ionisation, but leave open the consideration of ionisation with excitation. The ionised asymptotic state $|\Phi_\alpha \mathbf{k}_\alpha\rangle$ corresponds to the breakup of the target state $|\Phi_\alpha\rangle$ into a singly-ionised target state $|\Phi_{n_\alpha}^+\rangle$ (which may be excited) and an ionised electron in the form of a Coulomb wave $|\mathbf{q}_\alpha\rangle$; that is,

$$|\Phi_\alpha \mathbf{k}_\alpha\rangle = |\Phi_{n_\alpha}^+ \mathbf{q}_\alpha \mathbf{k}_\alpha\rangle \,, \tag{61}$$

where the energy of the ionised asymptotic state is of the form

$$E = \epsilon_\alpha + \tfrac{1}{2}k_\alpha^2 = \epsilon_{n_\alpha}^+ + \tfrac{1}{2}q_\alpha^2 + \tfrac{1}{2}k_\alpha^2 \tag{62}$$

where $\epsilon_{n_\alpha}^+$ is the energy of the singly-ionised target state, and where $\frac{1}{2}q_\alpha^2$ is the energy of the Coulomb wave. It is important to note that in this formulation, the asymptotic state $|\Phi_\alpha \mathbf{k}_\alpha\rangle$ separates into the asymptotic projectile state $|\mathbf{k}_\alpha\rangle$ and the asymptotic target state $|\Phi_\alpha\rangle = |\Phi_{n_\alpha}^+ \mathbf{q}_\alpha\rangle$, within which the Coulomb wave $|\mathbf{q}_\alpha\rangle$ is modelled - thus excluding from consideration a three-body boundary condition. This presents an issue however as Coulomb waves are not bounded states, and thus

their coordinate-space representations are not elements of $L^2(\mathbb{R}^3)$. This is the space wherein the coordinate-space representations of the one-electron states, comprising the target pseudostates, are spanned in terms of the Laguerre basis, (1). However it can be shown, as discussed in [8], that while the projection of a continuum wave onto a N-dimensional Laguerre basis is only conditionally convergent as N increases, it is numerically stable. Hence, the numerically calculated ionisation amplitudes can be written in the form

$$\begin{aligned} f^{(N)}_{\alpha,i} = f^{(N)}_{n_\alpha,n_i}(\mathbf{k}_\alpha,\mathbf{q}_\alpha,\mathbf{k}_i) &= \langle \mathbf{k}_\alpha \mathbf{q}_\alpha \Phi^+_{n_\alpha} | \hat{I}^{(N)}_T \hat{T} | \Phi^{(N)}_{n_i} \mathbf{k}_i \rangle \\ &= \sum_{n=1}^{N_T} \langle \mathbf{k}_\alpha \mathbf{q}_\alpha \Phi^+_{n_\alpha} | \Phi^{(N)}_n \rangle \, \langle \Phi^{(N)}_n | \hat{T} | \Phi^{(N)}_{n_i} \mathbf{k}_i \rangle \\ &= \sum_{n=1}^{N_T} \langle \mathbf{q}_\alpha \Phi^+_{n_\alpha} | \Phi^{(N)}_n \rangle \, \langle \mathbf{k}_\alpha \Phi^{(N)}_n | \hat{T} | \Phi^{(N)}_{n_i} \mathbf{k}_i \rangle \, . \end{aligned} \tag{63}$$

However, this expression is problematic as it involves a summation over not necessarily on-shell terms $\langle \mathbf{k}_\alpha \Phi^{(N)}_n |$. If we restrict our attention to only evaluating the ionisation amplitudes $f^{(N)}_{\alpha,i}$ for ionised asymptotic states $|\Phi^+_{n_\alpha} \mathbf{q}_\alpha \mathbf{k}_\alpha \rangle$ for which the ionised target energy satisfies

$$\epsilon_\alpha = \epsilon^+_{n_\alpha} + \tfrac{1}{2} q^2_\alpha = \epsilon^{(N)}_{n_\alpha}, \tag{64}$$

for one of the target pseudoenergies $\epsilon^{(N)}_{n_\alpha}$, corresponding to the target pseudostate $|\Phi^{(N)}_{n_\alpha}\rangle$, then we must have that

$$\langle \mathbf{q}_\alpha \Phi^+_{n_\alpha} | \Phi^{(N)}_n \rangle = \delta_{n_\alpha,n} \, \langle \mathbf{q}_\alpha \Phi^+_{n_\alpha} | \Phi^{(N)}_n \rangle \, , \tag{65}$$

whence the ionisation amplitudes can be evaluated as

$$f^{(N)}_{n_\alpha,n_i}(\mathbf{k}_\alpha,\mathbf{q}_\alpha,\mathbf{k}_i) = \langle \mathbf{q}_\alpha \Phi^+_{n_\alpha} | \Phi^{(N)}_{n_\alpha} \rangle \, \langle \mathbf{k}_\alpha \Phi^{(N)}_{n_\alpha} | \hat{T} | \Phi^{(N)}_{n_i} \mathbf{k}_i \rangle \, , \tag{66}$$

at these q_α which satisfy (64).

However, we note that a consequence of the assumed separability of the asymptotic state in (45) is that the anti-symmetrisation of the asymptotic state is neglected. Clearly this cannot be entirely neglected in the case of ionisation resulting in two unbounded electron states, even if one is screened by the other. Inclusion of the anti-symmetrisation of the ionised asymptotic state, with respect to the two unbounded electron states, results in the transformation

$$|\Phi^+_{n_\alpha} \mathbf{q}_\alpha \mathbf{k}_\alpha \rangle \mapsto [1 - \hat{P}_{0,n_e}] \, |\Phi^+_{n_\alpha} \mathbf{q}_\alpha \mathbf{k}_\alpha \rangle = |\Phi^+_{n_\alpha} \mathbf{q}_\alpha \mathbf{k}_\alpha \rangle - e^{\mathrm{i}\theta_\alpha} \, |\Phi^+_{n_\alpha} \mathbf{k}_\alpha \mathbf{q}_\alpha \rangle \, , \tag{67}$$

where $\theta_\alpha \in \{0, \pi\}$ is the exchange phase, corresponding to the exchange of the projectile and ionised electron states. Whence, as described in [4, 5, 9], we perform an ad-hoc anti-symmetrisation of the ionisation amplitude to account for this, resulting in a corrected ionisation amplitude $F^{(N)}_{n_\alpha,n_i}$ of the form

$$F^{(N)}_{n_\alpha,n_i}(\mathbf{k}_\alpha,\mathbf{q}_\alpha,\mathbf{k}_i) = f^{(N)}_{n_\alpha,n_i}(\mathbf{k}_\alpha,\mathbf{q}_\alpha,\mathbf{k}_i) - e^{-\mathrm{i}\theta_\alpha} f^{(N)}_{n_\alpha,n_i}(\mathbf{q}_\alpha,\mathbf{k}_\alpha,\mathbf{k}_i), \tag{68}$$

which satisfies

$$F^{(N)}_{n_\alpha,n_i}(\mathbf{k}_\alpha,\mathbf{q}_\alpha,\mathbf{k}_i) = -e^{-\mathrm{i}\theta_\alpha} F^{(N)}_{n_\alpha,n_i}(\mathbf{q}_\alpha,\mathbf{k}_\alpha,\mathbf{k}_i). \tag{69}$$

We note that in the CCC method, we refer to $f^{(N)}_{\alpha,i}$ simply as the ionisation amplitudes (or as the unsymmetrised ionisation amplitudes when specificity is required), and we refer to $F^{(N)}_{\alpha,i}$ as the anti-symmetrised ionisation amplitudes. We note that while the anti-symmetrised ionisation amplitudes

are used for comparison with experimental results, we make reference to the unsymmetrised ionisation amplitudes in the discussion of ionisation in the CCC method. Lastly, we note that we are constrained to evaluating these amplitudes only for a countable number of outgoing projectile energies, bound by the constraint defined in (64). Evaluating the ionisation scattering amplitudes at any other energy requires an interpolation between these energies.

2.2.2 Cross-Sections

We present expressions for the partial and total cross sections, in a manner similar to [8, 10]. In general terms, the partial cross sections are of the form

$$\sigma_{\alpha,\beta} = \sigma_{\alpha,\beta}(\mathbf{k}_\alpha, \mathbf{k}_\beta) = \frac{k_\alpha}{k_\beta}|f_{\alpha,\beta}|^2 = \frac{k_\alpha}{k_\beta}|\,\langle \mathbf{k}_\alpha \Phi_\alpha | \hat{T} | \Phi_\beta \mathbf{k}_\beta \rangle|^2, \tag{70}$$

with the specific notation for elastic, discrete excitation, and ionisation cross sections paralleling the notation used in (58), (60), and (63) respectively.

The total cross section (TCS), for a given initial asymptotic state, is obtained as a sum of all partial cross sections for which the outgoing asymptotic projectile energy is positive,

$$\sigma^{(N)}_{\mathrm{T};i} = \sum_{f:k_f>0} \sigma^{(N)}_{f,i}, \tag{71}$$

while the total ionisation cross section (TICS), for a given initial asymptotic state, is obtained as a sum of all partial cross sections for which the outgoing asymptotic projectile and target energies are positive (and thus unbounded),

$$\sigma^{(N)}_{\mathrm{I};i} = \sum_{\alpha:k_\alpha>0,\epsilon^{(N)}_\alpha>0} \sigma^{(N)}_{\alpha,i}. \tag{72}$$

An ionisation cross section can also be constructed for a particular outgoing asymptotic ionised target state by an appropriate restriction of the sum in (72),

$$\sigma^{(N)}_{\mathrm{I};n_f,i} = \sum_{\alpha:k_\alpha>0,\epsilon^{(N)}_\alpha>0,n_\alpha=n_f} \sigma^{(N)}_{\alpha,i}. \tag{73}$$

We also consider the various differential cross sections in the context of ionisation transitions, following in the form of [25]. Evaluating the partial cross sections, for an ionisation transition, yields the triple-differential cross section (TDCS),

$$\frac{\mathrm{d}\sigma^{(N)}_{\alpha,i}}{\mathrm{d}\Omega_{k_\alpha}\,\mathrm{d}\Omega_{q_\alpha}\,\mathrm{d}e_{q_\alpha}}(\mathbf{k}_\alpha, \mathbf{q}_\alpha, \mathbf{k}_i) = \frac{k_\alpha q_\alpha}{k_i}|F^{(N)}_{n_\alpha,n_i}(\mathbf{k}_\alpha, \mathbf{q}_\alpha, \mathbf{k}_i)|^2, \tag{74}$$

where $e_{q_\alpha} = \frac{1}{2}q_\alpha^2 \in [0, E - \epsilon^+_{n_\alpha}]$ is the energy of the outgoing projectile electron, and where $\Omega = (\theta, \phi)$ refers to the spherical coordinates of momentum-space. Integrating the TDCS over the spherical coordinates of either the outgoing asymptotic projectile electron, or the outgoing ionised target electron, yields the double-differential cross section (DDCS). Furthermore, integrating the DDCS over the spherical coordinates of the remaining electron, whichever one that may be, yields the single-differential cross section (SDCS), which is of the form

$$\frac{\mathrm{d}\sigma^{(N)}_{\alpha,i}}{\mathrm{d}e_{q_\alpha}}(e_{q_\alpha}) = \frac{k_\alpha q_\alpha}{k_i}\int_{S^2}\mathrm{d}\Omega_{k_\alpha}\int_{S^2}\mathrm{d}\Omega_{q_\alpha}\,|F^{(N)}_{n_\alpha,n_i}(\mathbf{k}_\alpha, \mathbf{q}_\alpha, \mathbf{k}_i)|^2, \tag{75}$$

where we recall that the energies of the incoming and outgoing projectile states, as well as the ionised electron state, are constrained to be on-shell as specified in (62). Integration of the SDCS over the projectile (or target) electron energy yields the total ionisation cross section.

2.3 Considerations for a Helium Target

We briefly remark on some of the specific considerations needed for a helium target, in the CCC method. We recall, from Equation 15, that the target psuedostates $\{ |\Phi_n^{(N)}\rangle \}_{n=1}^{N_T}$ are constructed by expanding the target Hamiltonian $\hat{H}_T$ in a basis, formed from a selection of Slater determinants, and diagonalising. For the case of a helium target, these Slater determinants assume the form

$$\left\{ |\chi_{[a_1,a_2]}^{(N)}\rangle : a_1, a_2 \in \{1, \ldots, 2N\} \right\}, \tag{76}$$

and we recall their anti-symmetric properties,

$$|\chi_{[a_2,a_1]}^{(N)}\rangle = -\,|\chi_{[a_1,a_2]}^{(N)}\rangle \quad , \quad |\chi_{[a_1,a_1]}^{(N)}\rangle = 0$$

for $a_1, a_2 \in \{1, \ldots, 2N\}$. The helium target pseudostates will be expressed in the form

$$|\Phi_n^{(N)}\rangle = \sum_{a_1=1}^{2N} \sum_{a_2>a_1}^{2N} D_n^{a_1,a_2} \, |\chi_{[a_1,a_2]}^{(N)}\rangle \tag{77}$$

for $n = 1, \ldots, N_T$, where $D_n^{a_1,a_2}$ are the coefficients of the expansion. As mentioned earlier in section 2.1.2, we restrict our selection of Slater determinants to those for which the first (core) orbital ranges over a smaller set of spin orbitals, $\{ |\chi_i^{(N)}\rangle \}_{i=1}^{2C}$ defined by the parameter $C \leq N$, while placing no such restriction on the second (valence) orbital, yielding target pseudostates of the form

$$|\Phi_n^{(C,N)}\rangle = \sum_{a_1=1}^{2C} \sum_{a_2>a_1}^{2N} D_n^{a_1,a_2} \, |\chi_{[a_1,a_2]}^{(N)}\rangle \, . \tag{78}$$

We also note that the target pseudostates, when expanded in the basis of Slater determinants, are often dominated by a single term. With this in mind, we say that the dominating Slater determinant is the major configuration of a particular target pseudostate, and we define the major configuration coefficient as the absolute value of the associated expansion coefficient.

3 Results

3.1 Convergence Strategy

With the aim of calculating convergent TICS for helium using the CCC method, we first establish how convergence is to be achieved. The parameters which most uniquely define our CCC calculations are:

N the number of one-electron atomic orbitals used in the construction of the target pseudostates; equivalently, the number of Laguerre basis states,

C the number of core states; that is, the number of one-electron atomic orbitals that may be used for the core orbitals of the configurations used to construct the target pseudostates,

λ the exponential fall-off parameter of the Laguerre basis.

Hence, we denote a CCC calculation performed with a particular selection of values for these parameters by $\mathrm{CCC}(C, N, \lambda)$.

We recall that the parameter $C \in \{1, \ldots, N\}$ essentially acts to restrict the number of configurations available for the representation of target pseudostates as linear combinations of configurations. We also recall that the parameter C acts only on the core orbitals, while the valence orbitals retain the use of all available one-electron atomic orbitals. The projectile electron will interact with both the core and valence electrons in the helium target during the scattering process, but we expect the valence electron to play a more significant role in these interactions. As a result, we expect that doubly-excited configurations with higher excitations of the core orbital will have diminishing influence in the scattering processes. Furthermore, we expect the accuracy of the calculations to increase diminishingly as the parameter C increases. Hence, for fixed values of the parameters N and λ, we expect that the calculations will converge with regard to parameter C, in the sense of

$$\mathrm{CCC}(N, \lambda) = \lim_{C \to N} \mathrm{CCC}(C, N, \lambda).$$

We then sought to obtain convergence with regard to parameter N, with the role of the parameter λ initially assumed to be supplemental. However, as discussed further in subsection 3.4, the effect of these parameters on the TICS calculations proved to be more nuanced.

We also recall now that the number of target pseudostates used in the calculation $\mathrm{CCC}(C, N, \lambda)$ scales as $\mathcal{O}(N_T) = CN$, with the parameter $C \in \{1, \ldots, N\}$. As a consequence, it is often computationally impractical to perform more than a few calculations of the form $\{\mathrm{CCC}(C, N, \lambda) : C = 1, 2, \ldots\}$. This is balanced by the fact that the TICS for these calculations tended to converge sufficiently by $C = 6$.

With this in mind, we make clear that we will be presenting two sets of CCC calculations:

- sets of $\mathrm{CCC}(C, N, 0.5)$ calculations for $N \in \{20, 25, 30, 35, 40, 50\}$ and $C \in \{2, \ldots, 6\}$, with the larger N calculations having smaller maximum values for the parameter C,
- a set of $\mathrm{CCC}(2, 35, \lambda)$ calculations for $\lambda \in \{0.40, 0.41, \ldots, 0.65\}$.

The first set of calculations is presented for the analysis of convergence of the total ionisation cross sections, while the second is presented for a deeper analysis of the helium target pseudostates.

3.2 TICS-without-Excitation

We present the CCC$(C, 35, 0.5)$ calculations of the total cross section for electon-impact ionisation-without-excitation of helium in Figure 1, and again confirm [19, 22] the agreement between CCC and PECS calculations of this cross section. Convergence was similarly achieved in CCC$(C, N, 0.5)$ calculations with $N \in \{20, 25, 30, 40, 50\}$, and so are not presented here to avoid duplicity.

A point of interest, however, is that the CCC cross sections consistently have a smaller flux across the intermediate energy range than the PECS cross sections. This suggests that the total ionisation-without-excitation cross section may have an amount of flux siphoned away, namely into the total ionisation-with-excitation cross sections, in the CCC calculations, as will be discussed with more evidence further on.

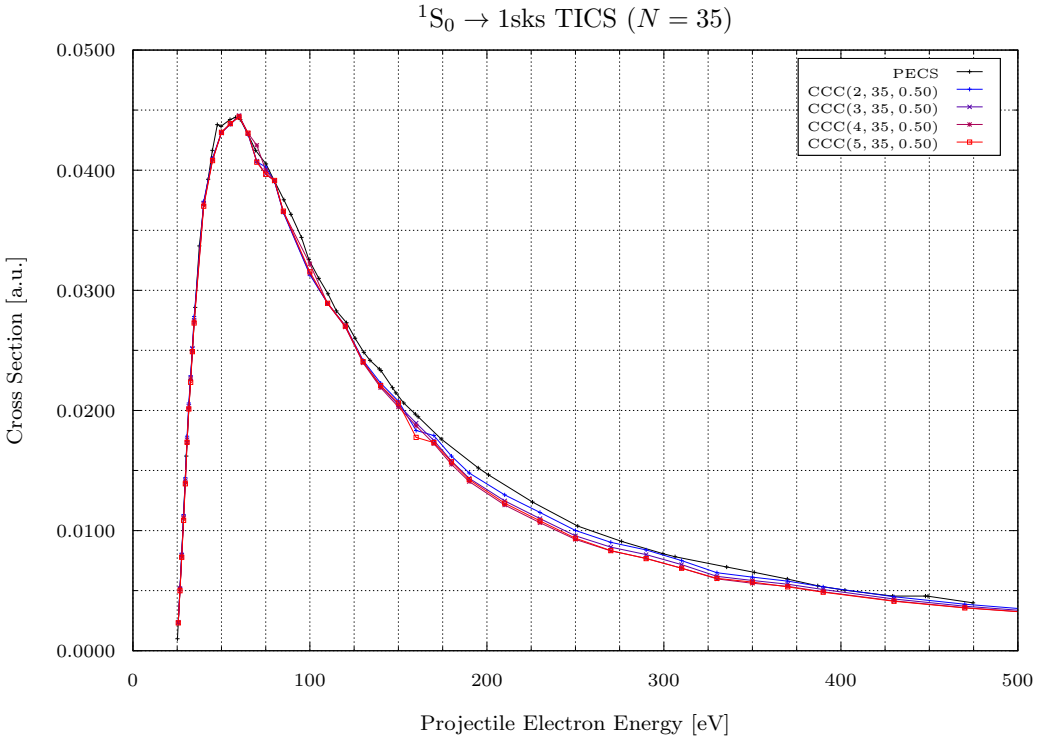

Figure 1: Total cross sections for electron-impact ionisation-without-excitation of helium, leaving the helium ion in a 1s state. CCC(C, N, λ) calculations, with $N = 35$ and $\lambda = 0.50$, are presented for $C = 2, \ldots, 5$, and are compared with PECS [22] calculations.

3.3 TICS-with-Excitation

With the aim of rectifying the CCC calculations by seeking agreement with the PECS calculations [22] for the total cross section for electron-impact ionisation-with-excitation of helium, we have restricted our consideration to the cross sections which leave the helium ion in a 2s state. This is sufficient to examine the effects of auto-ionisation on the ionisation-with-excitation cross sections in general.

We present the CCC($C, N, 0.5$) calculations of the total cross section for electron-impact ionisation-with-excitation of helium (leaving the helium ion in a 2s state), taken for increasing values of the parameter C until either convergence or computational limits are found, for: $N = 20$ in Figure 2, $N = 25$ in Figure 3, $N = 30$ in Figure 4, $N = 35$ in Figure 5, $N = 40$ in Figure 6, $N = 50$ in Figure 7.

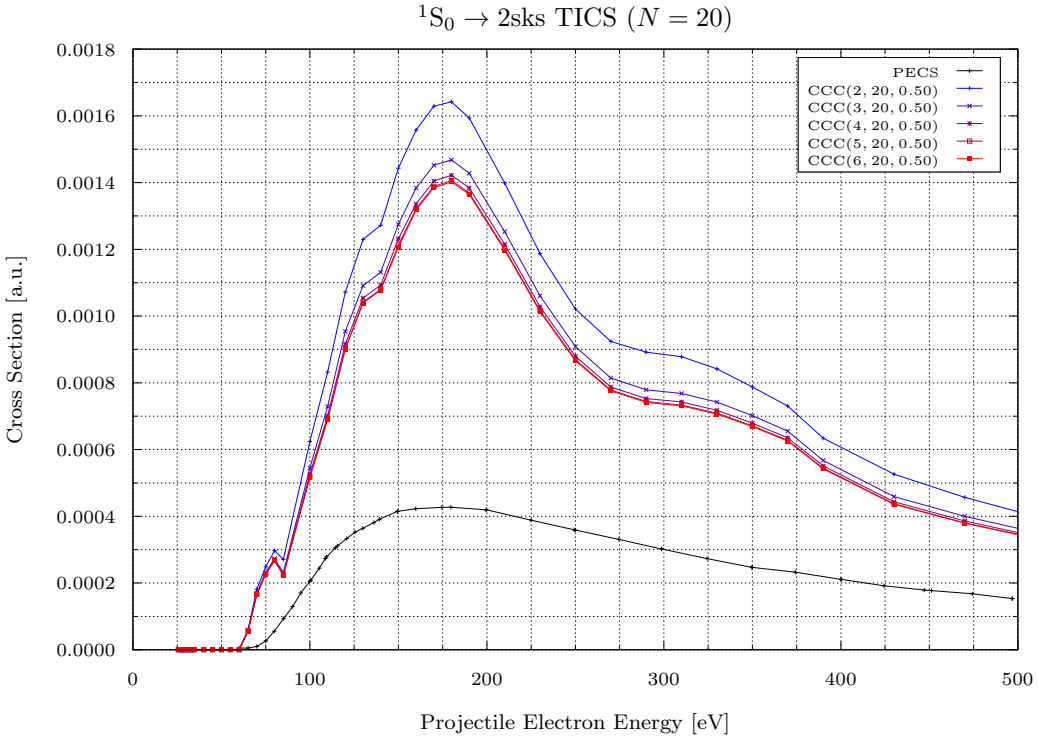

Figure 2: Total cross sections for electron-impact ionisation-with-excitation of helium, leaving the helium ion in a 2s state. CCC(C, N, λ) calculations, with $N = 20$ and $\lambda = 0.50$, are presented for $C = 2, \ldots, 6$, and are compared with PECS [22] calculations.

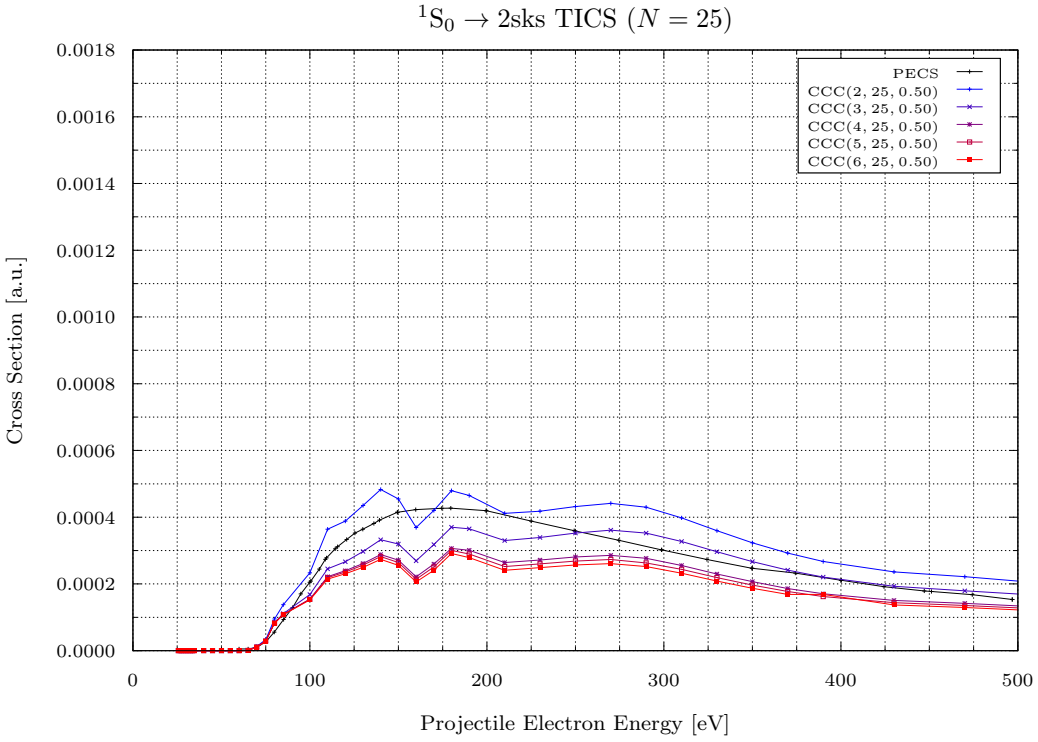

Figure 3: Total cross sections for electron-impact ionisation-with-excitation of helium, leaving the helium ion in a 2s state. CCC(C, N, λ) calculations, with $N = 25$ and $\lambda = 0.50$, are presented for $C = 2, \ldots, 6$, and are compared with PECS [22] calculations.

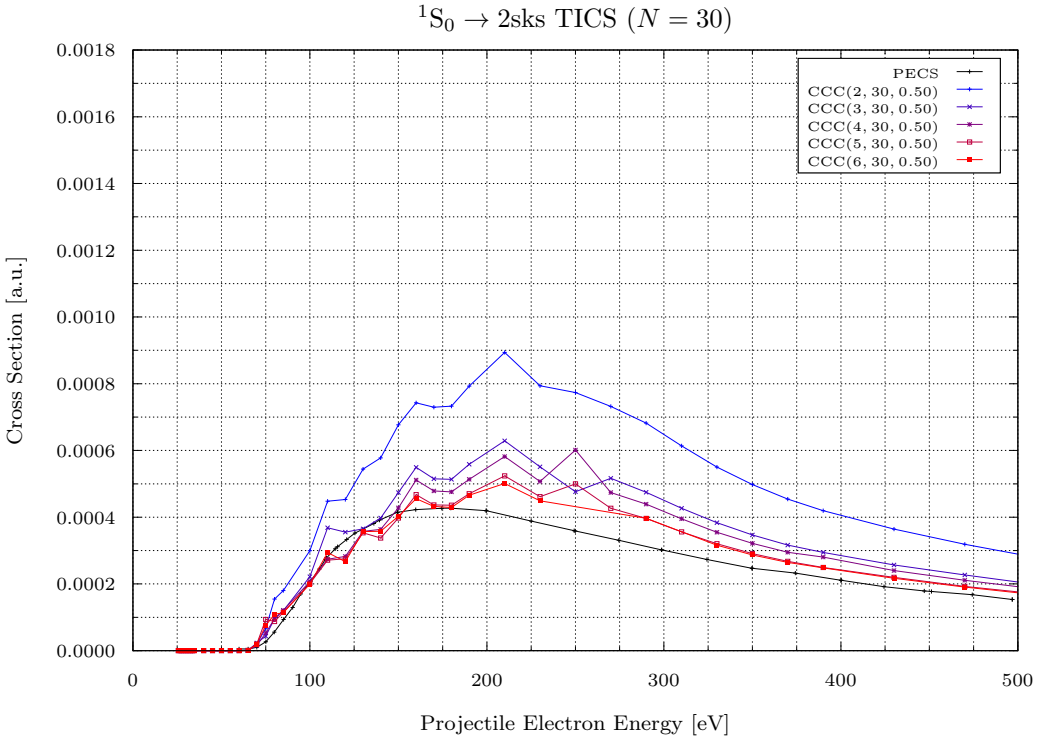

Figure 4: Total cross sections for electron-impact ionisation-with-excitation of helium, leaving the helium ion in a 2s state. CCC(C, N, λ) calculations, with $N = 30$ and $\lambda = 0.50$, are presented for $C = 2, \ldots, 6$, and are compared with PECS [22] calculations.

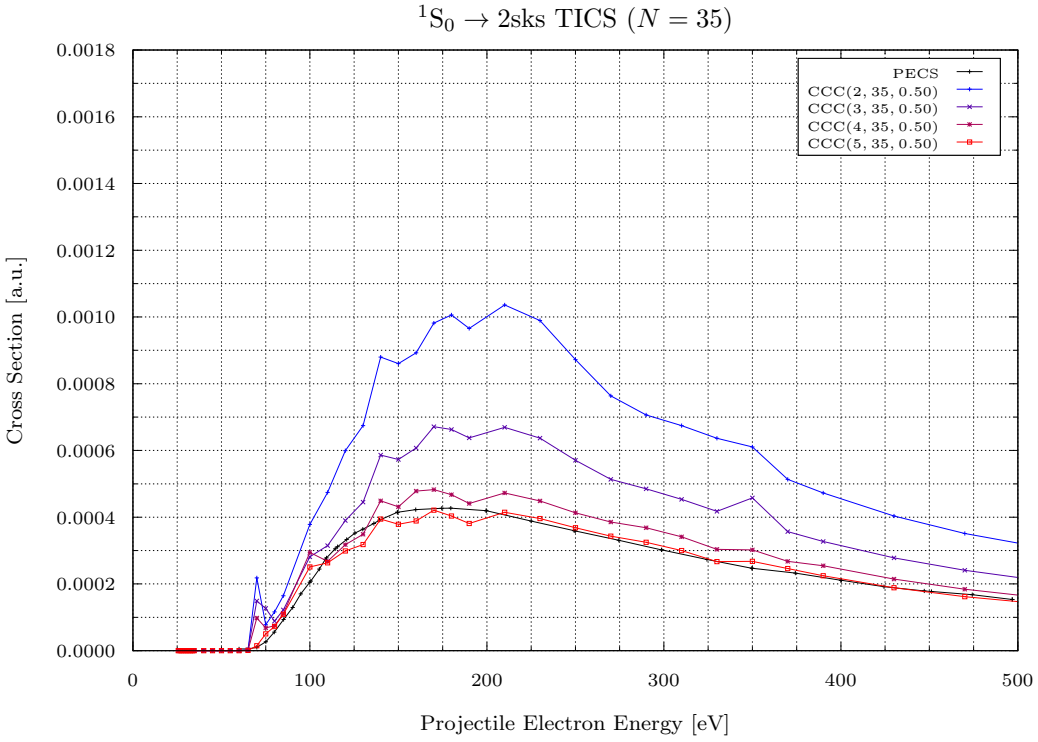

Figure 5: Total cross sections for electron-impact ionisation-with-excitation of helium, leaving the helium ion in a 2s state. CCC(C, N, λ) calculations, with $N = 35$ and $\lambda = 0.50$, are presented for $C = 2, \ldots, 5$, and are compared with PECS [22] calculations.

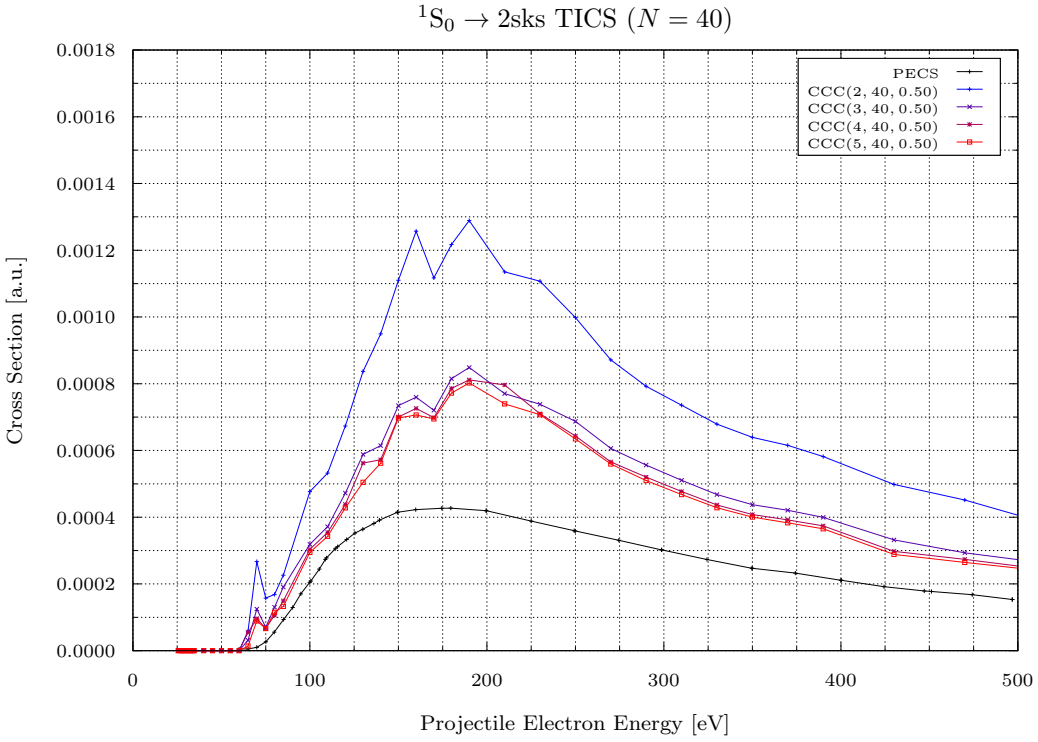

Figure 6: Total cross sections for electron-impact ionisation-with-excitation of helium, leaving the helium ion in a 2s state. CCC(C, N, λ) calculations, with $N = 40$ and $\lambda = 0.50$, are presented for $C = 2, \ldots, 5$, and are compared with PECS [22] calculations.

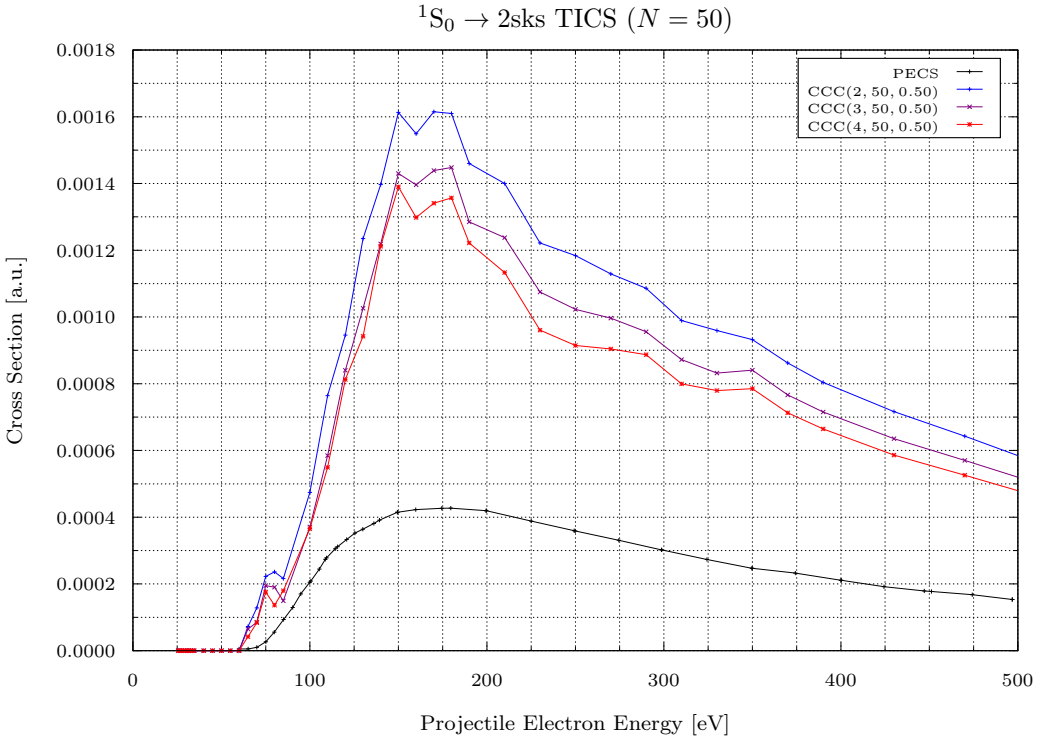

Figure 7: Total cross sections for electron-impact ionisation-with-excitation of helium, leaving the helium ion in a 2s state. CCC(C, N, λ) calculations, with $N = 50$ and $\lambda = 0.50$, are presented for $C = 2, \ldots, 4$, and are compared with PECS [22] calculations.

It can be seen that the cross sections do indeed demonstrate convergence, for each value of the parameter N, with increasing values of the parameter C, typically by $C = 6$; that is, that they converge in the sense of

$$\mathrm{CCC}(N, \lambda) = \lim_{C \to N} \mathrm{CCC}(C, N, \lambda).$$

However, it can also be seen that the successive cross sections do not demonstrate convergence with regard to the parameter N; that is, in the sense of

$$\mathrm{CCC}(\lambda) = \lim_{N \to \infty} \mathrm{CCC}(N, \lambda).$$

Both the magnitude, and to an extent - the form, of the cross sections vary quite substantially between different values of N, dismissing the possibility of bringing these cross sections to converge with brute force.

While a few of these cross sections do in fact demonstrate a level of agreement with the PECS calculations, they do not do so in a consistent manner. On the other hand, it is somewhat reassuring that the majority of the cross sections are within one order-of-magnitude of the PECS calculations, and so should not be rejected as entirely flawed. We do note, however, the tendency for the CCC cross sections to be larger than the PECS cross section, especially in the intermediate energy range.

A comparison of the CCC$(5, 35, 0.5)$ calculations, alongside the PECS calculations, for the total ionisation-without-excitation and ionisation-with-excitation cross sections is presented in Figure 8, with the ionisation-with-excitation cross section scaled up by a factor of 10. This indicates with clarity the substantial difference in magnitude between these cross sections. Furthermore, it demonstrates that where the CCC ionisation-without-excitation cross sections tend to have less flux than the PECS calculation, the CCC ionisation-with-excitation cross sections tend to have more flux than the PECS calculations.

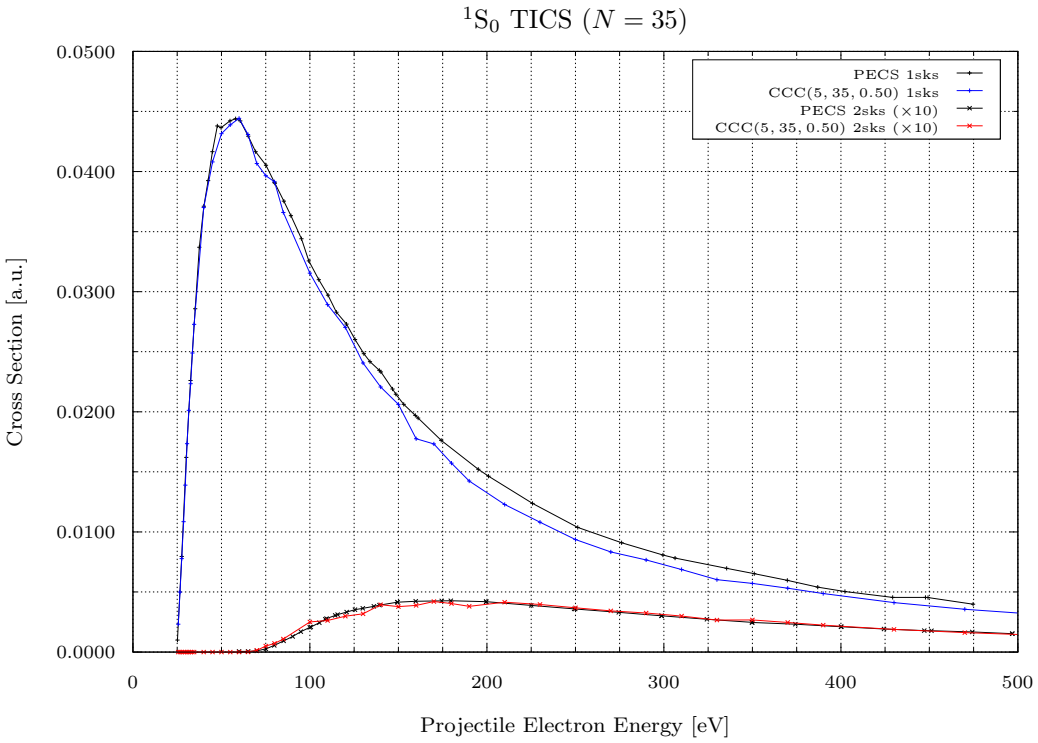

Figure 8: Total cross sections for electron-impact ionisation-without-excitation (1sks) and ionisation-with-excitation (2sks) of helium. CCC(C, N, λ) calculations, with $C = 5$, $N = 35$ and $\lambda = 0.50$, are presented and compared with PECS [22] calculations. Note that for clarity, the ionisation-with-excitation (2sks) cross sections are presented scaled up by a factor of 10.

3.4 Mixed Target States

At this point, we put forward our suspicion regarding the discrepancies observed between the CCC and PECS calculations of the total cross section for electron-impact ionisation-with-excitation of helium: that they are the result of the helium target pseudostates being mixed states, in the CCC calculations. Specifically, that as the discrete doubly-excited & continuum ionised-with-excitation helium states, and the continuum of ionised-without-excitation helium states have overlapping energy spectrums, the helium target pseudostates often are constructed as mixed combinations of two configurations - one from each spectrum. This will then cause a predominantly doubly-excited or ionised-with-excitation helium state, but with a non-negligble ionised-without-excitation component, to contribute the flux of the ionised-without-excitation term to the ionised-with-excitation cross section, while also removing that flux from the ionised-without-excitation cross section. Furthermore, as the flux associated with the ionised-without-excitation states is significantly larger than that associated with the doubly-excited states & ionised-with-excitation states, the mixing of states would disproportionately effect the ionisation-with-excitation cross section. Thus, mixed helium pseudostates would explain the reduced flux of the CCC ionisation-without-excitation cross sections - and the increased flux of the ionisation-with-excitation cross sections - in comparison with the PECS calculations.

We briefly discuss mixed target states in further detail, to make this discussion more precise. Ideally, the target pseudostates would be purely one configuration, if sufficiently appropriate one-electron atomic orbitals are selected to construct the configurations; that is, where $|\Phi_n^{(C,N)}\rangle$ is any such pure pseudostate, it would have a major configuration coefficient of $D_n^{a_1,a_2} \approx 1$ for some particular a_1, a_2, and would be of the form

$$|\Phi_n^{(C,N)}\rangle = \sum_{a_1=1}^{2C} \sum_{a_2>a_1}^{2N} D_n^{a_1,a_2} \, |\chi_{[a_1,a_2]}^{(N)}\rangle \approx |\chi_{[a_1,a_2]}^{(N)}\rangle \, .$$

However, in the case where two pseudostates, $|\Phi_n^{(C,N)}\rangle$ and $|\Phi_{n'}^{(C,N)}\rangle$, each with a major configuration, $|\chi_{[a_1,a_2]}^{(N)}\rangle$ and $|\chi_{[a_1',a_2']}^{(N)}\rangle$, have converging pseudoenergies, they will increasingly tend to being constructed as mixed combinations of each configuration, in the form

$$\begin{pmatrix} |\Phi_n^{(C,N)}\rangle \\ |\Phi_{n'}^{(C,N)}\rangle \end{pmatrix} = \begin{pmatrix} D_n^{a_1,a_2} & D_n^{a_1',a_2'} \\ D_{n'}^{a_1,a_2} & D_{n'}^{a_1',a_2'} \end{pmatrix} \begin{pmatrix} |\chi_{[a_1,a_2]}^{(N)}\rangle \\ |\chi_{[a_1',a_2']}^{(N)}\rangle \end{pmatrix} .$$

The doubly-excited states of helium do in fact have energies which are contained within the continuum of energies associated with ionised-without-excitation states of helium, in addition to the overlapping nature of the ionised-with-excitation and ionised-without-excitation energy spectrums, and hence it is possible to have distinct target pseudostates with near equal pseudoenergies.

Furthermore, the configurations are constructed using the one-electron atomic orbitals, which are parameterised by the exponential fall-off factor λ. A well-observed effect of this parameter is to continuously adjust the energies of the discretised continuum one-electron atomic-orbitals. It follows that as the value of λ is adjusted, we would expect the pseudoenergies of configurations with continuum orbitals to continuously shift also, while the pseudoenergies of discrete configurations would remain constant; in a sense, sweeping across the static discrete energy levels. Additionally, the pseudoenergies of the configurations associated with ionised-without-excitation and ionised-with-excitation will vary with λ distinctly. Consequently, we should expect various pairs of ionisied-without-excitation and doubly-excited or ionisied-with-excitation target pseudostates to overlap in

energy as λ is adjusted, and thus the mixing of these pairs of pseudostates. We would therefore expect the ionisation-with-excitation cross sections to vary dramatically with continuous changes in λ, and this is indeed demonstrated in Figure 9 with CCC$(2, 35, \lambda)$ calculations presented for $\lambda = 0.40, \ldots, 0.65$.

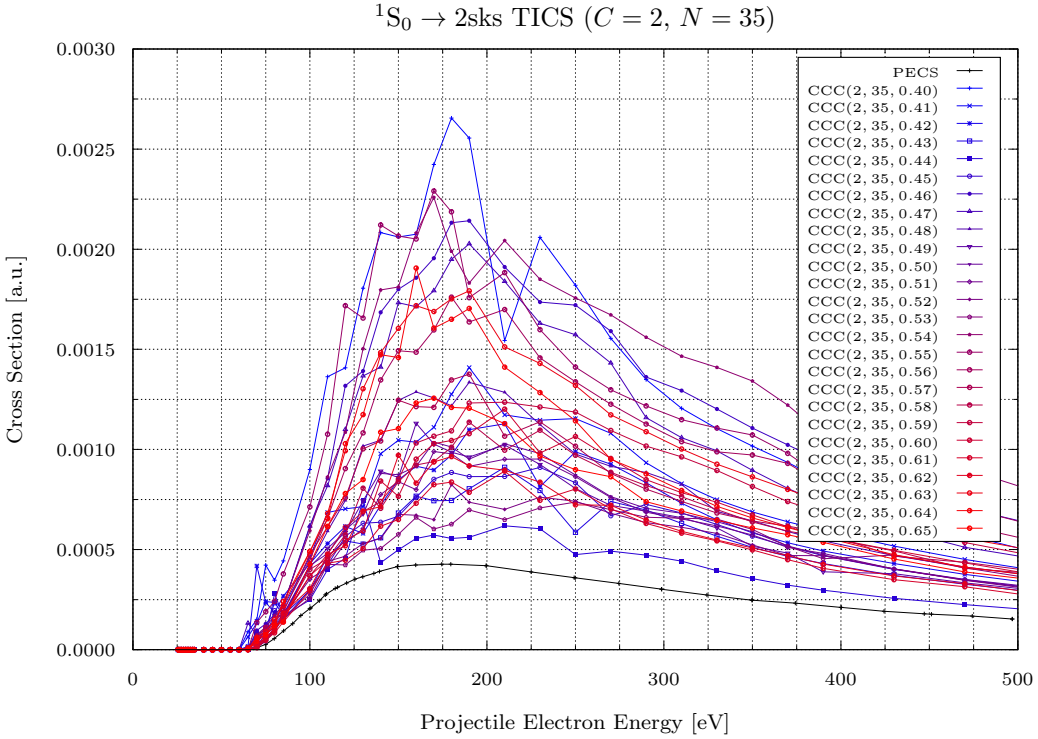

Figure 9: Total cross sections for electron-impact ionisation-with-excitation of helium, leaving the helium ion in a 2s state. CCC(C, N, λ) calculations, with $C = 2$ and $N = 35$, are presented for $\lambda = 0.40, 0.41, \ldots, 0.65$, and are compared with PECS [22] calculations.

We present the spectrums of helium pseudoenergies, constructed with the CCC$(2, 35, \lambda)$ calculations across the range of $\lambda = 0.40, \ldots, 0.65$, for singlet helium pseudostates in Figure 10 and for triplet helium pseudostates in Figure 11. We also present an alternative view of the spectrum of singlet helium pseudoenergies, in Figure 12, to more clearly present the pseudoenergies associated with auto-ionising helium states.

The discrete pseudoenergies associated with singly-excited, and doubly-excited configurations can be seen, and are distinguished by their tendency to remain constant with changes in λ. Furthermore, the continuum pseudoenergies associated with ionised-without-excitation and ionised-with-excitation configurations can also be seen, being distinguished by their tendency to vary continuously with λ. The pseudoenergies associated with ionised-without-excitation (1s) configurations are distinguishable from those associated with ionised-with-excitation (2s) configurations, by their larger rate of change with changes in λ.

Indeed, the behaviour predicted of the discrete and continuum spectrums of pseudoenergies is observed, as is the intersecting nature of the pseudoenergies associated with ionised-without-excitation states with the pseudoenergies of both doubly-excited states and ionised-with-excitation states.

Also of interest is the behaviour most clearly seen in Figure 12; that as the ionised-without-excitation pseudoenergies approach the pseudoenergy of either a discrete doubly-excited state, or a more slowly increasing ionised-with-excitation state, they swap configurations, passing on its more energetic behaviour onto the next state and taking on their less energetic behaviour.

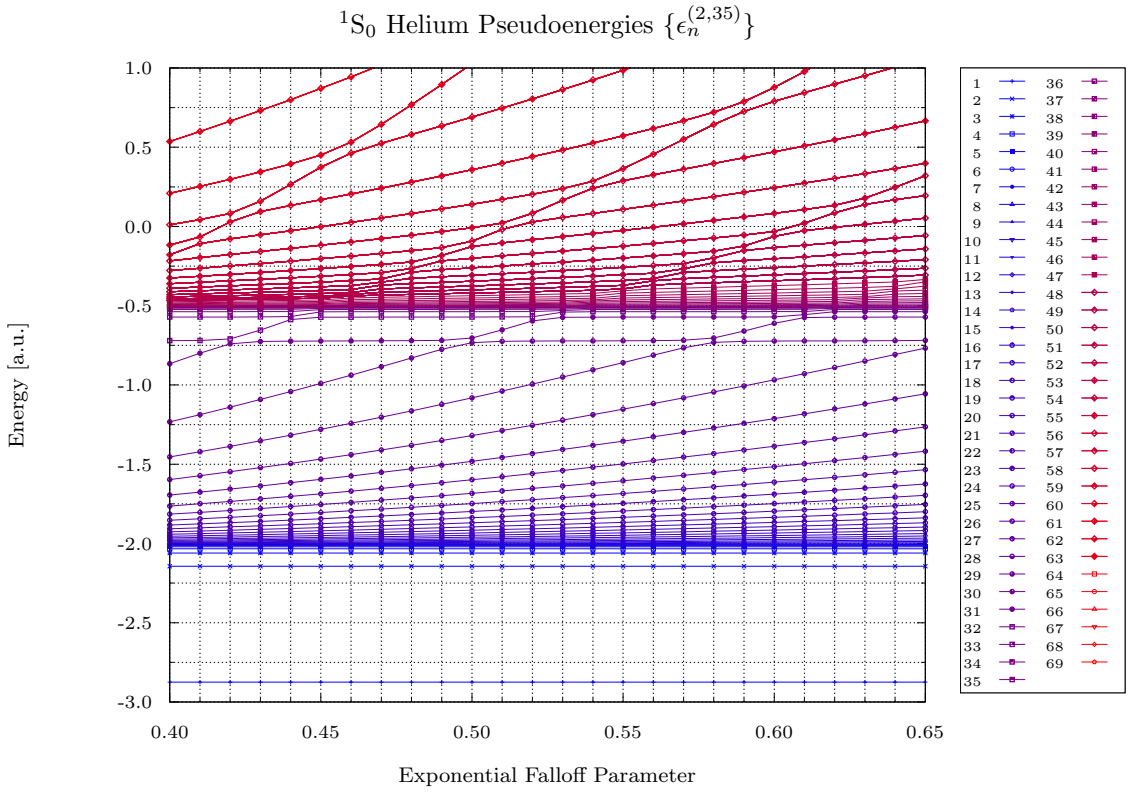

Figure 10: The spectrums of pseudoenergies corresponding to singlet helium pseudostates, calculated with $C = 2$ and $N = 35$, are presented for $\lambda = 0.40, 0.41, \ldots, 0.65$.

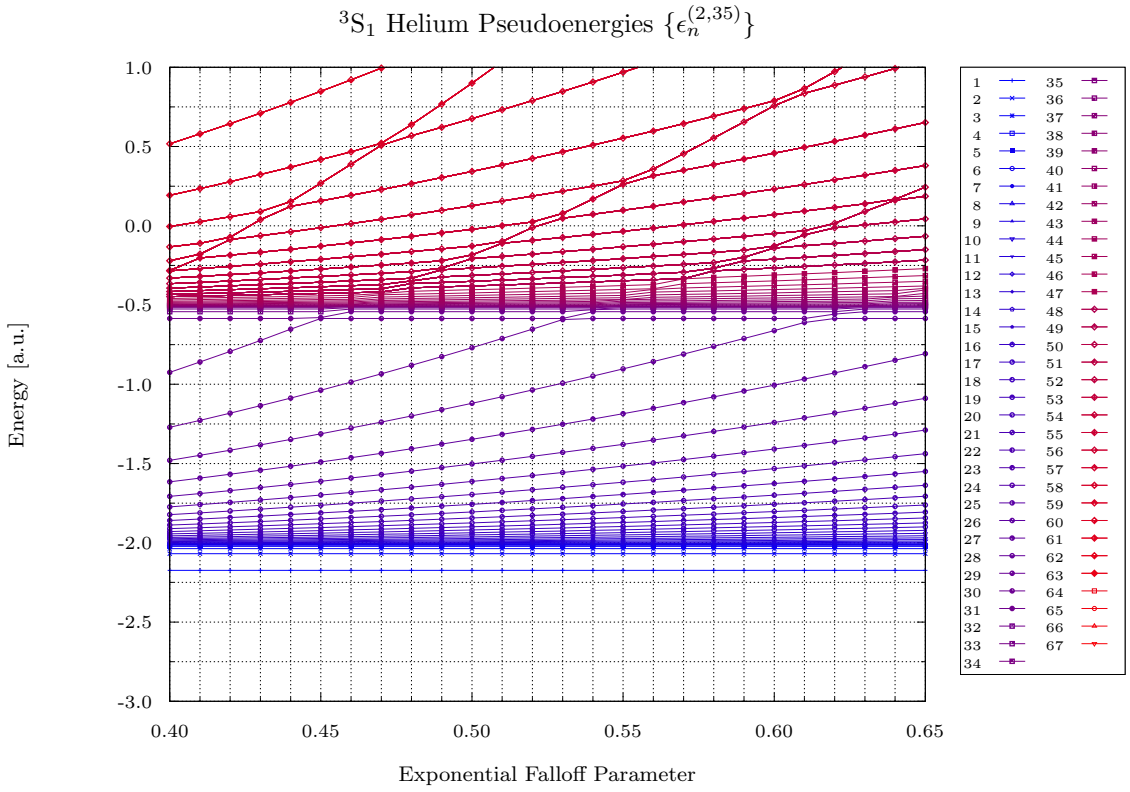

Figure 11: The spectrums of pseudoenergies corresponding to triplet helium pseudostates, calculated with $C = 2$ and $N = 35$, are presented for $\lambda = 0.40, 0.41, \ldots, 0.65$.

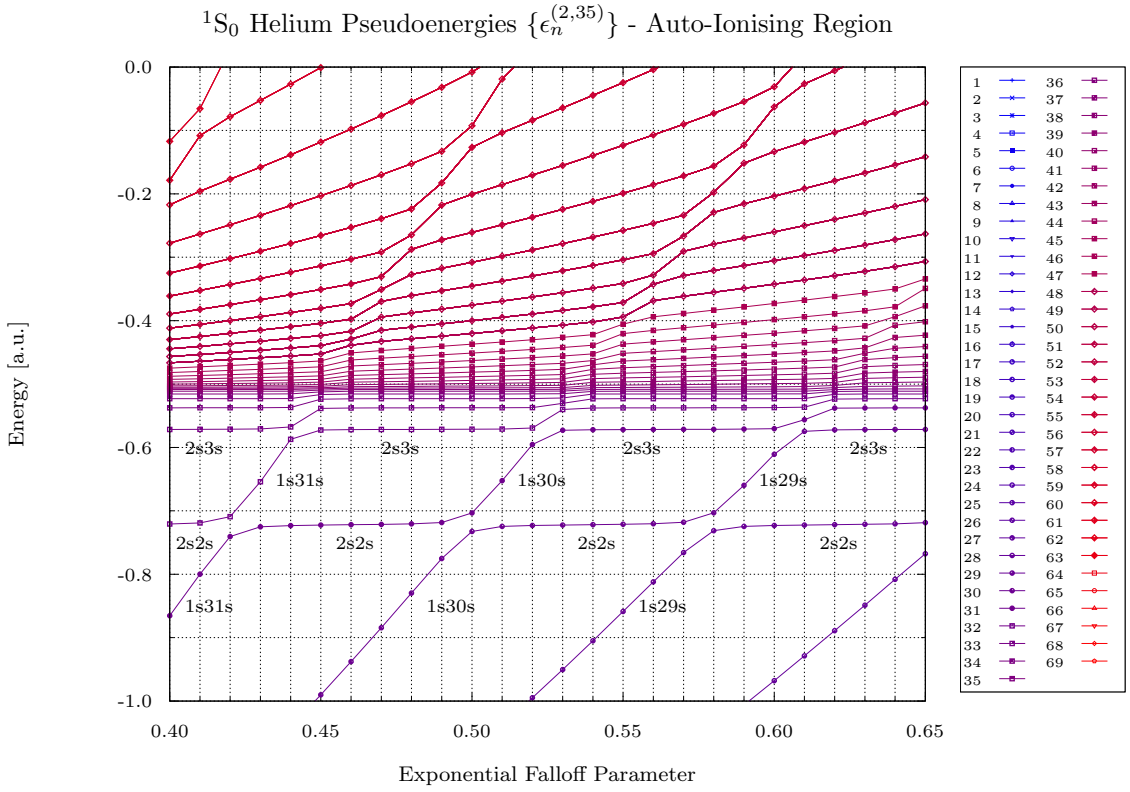

Figure 12: The same data is shown as in Figure 10, with the y-axis restricted to focus on the auto-ionising region, wherein discrete doubly-excited states overlap with continuum states. For clarity, a number of pseudoenergies are annotated by their corresponding major configuration across ranges of λ values, including discrete doubly-excited states (2s2s, 2s3s) and continuum states (1s29s, 1s30s, 1s31s).

To further exemplify the mixing of helium pseudostates and the effect it has on the ionisation cross sections, we present, for selected singlet pseudostates (and their energetic predecessor and successor), their major configuration coefficient and their partial cross sections (viewed orthographically), constructed with CCC$(2, 35, \lambda)$ calculations across the range of $\lambda = 0.40, \ldots, 0.65$. A pure pseudostate, $|\Phi_3^{(2,35)}\rangle$, is presented in Figure 13 and Figure 14. Pseudostates subjected to a larger degree of mixing are presented also: $|\Phi_{30}^{(2,35)}\rangle$ in Figure 15 and Figure 16, $|\Phi_{34}^{(2,35)}\rangle$ in Figure 17 and Figure 18, $|\Phi_{53}^{(2,35)}\rangle$ in Figure 19 and Figure 20.

Note that the partial cross sections have been presented orthographically, to focus on the magnitude of the cross sections rather than their particular form. This is done to demonstrate that while the partial cross sections of pure pseudostates exhibit fairly consistent magnitudes, the partial cross sections of mixed states vary in magnitude significantly as they adjust from one configuration into another; specifically, from an ionised-without-excitation configuration with a large magnitude to a doubly-excited or ionised-with-excitation configuration with a significantly smaller magnitude.

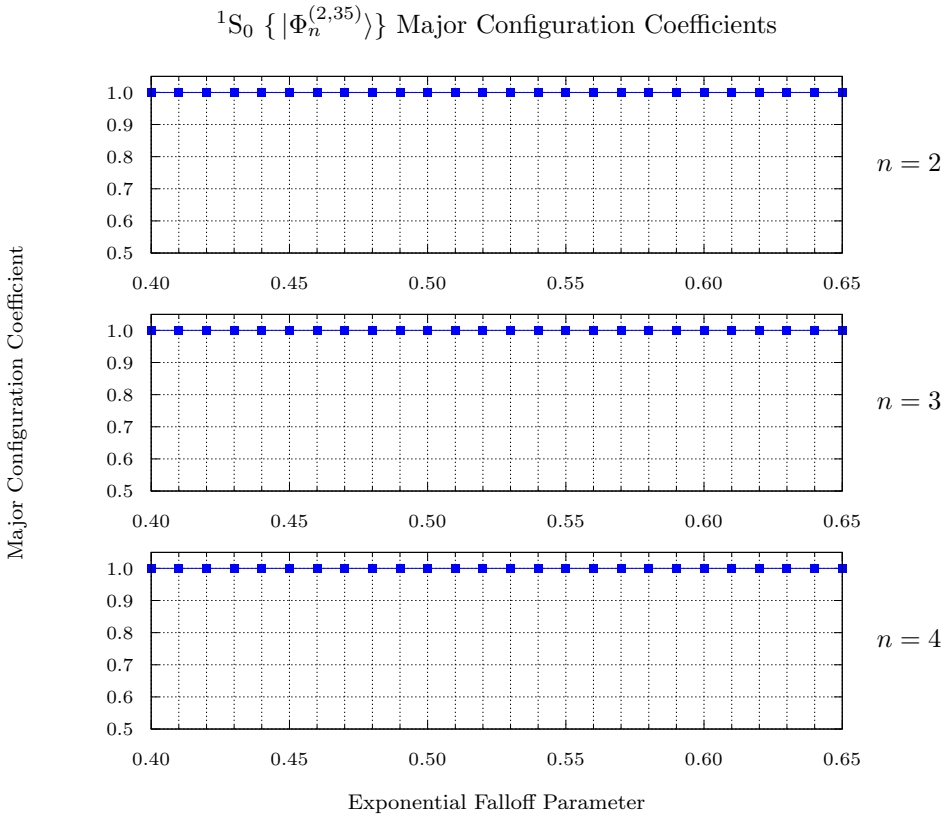

Figure 13: The major configuration coefficients of the singlet helium pseudostates, $|\Phi_n^{(C,N)}\rangle$ calculated with $C = 2$ and $N = 35$, are presented across a range of $\lambda = 0.40, 0.41, \ldots, 0.65$, for the states $n = 2, 3, 4$.

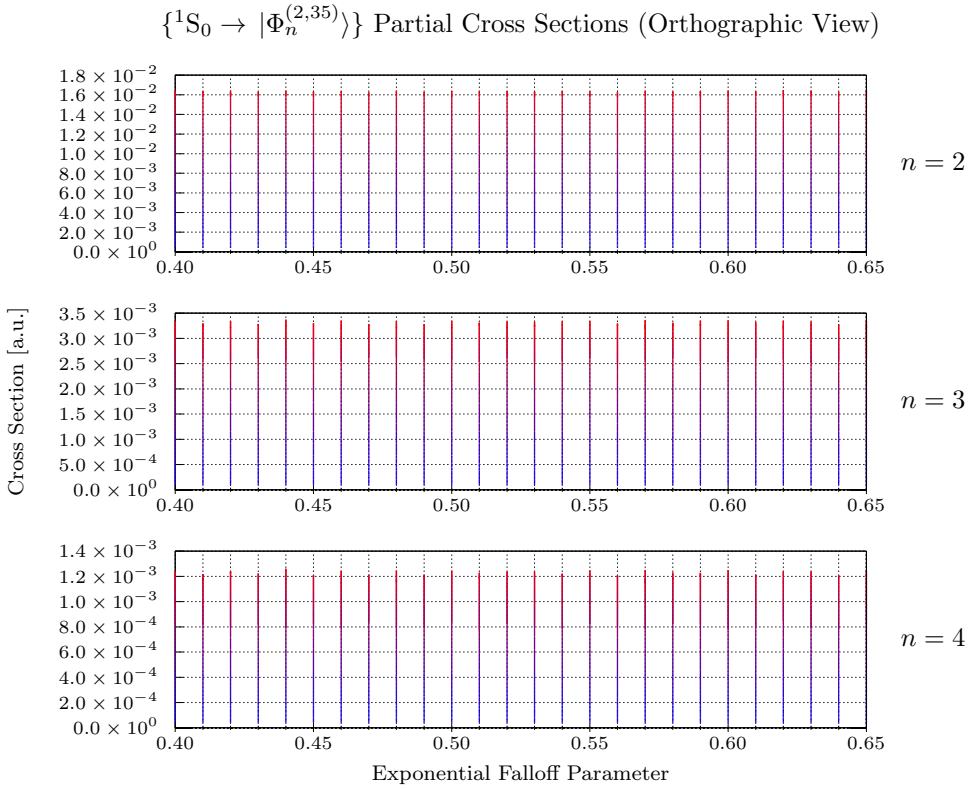

Figure 14: The partial cross sections of ground state singlet helium to the singlet pseudostates, $|\Phi_n^{(C,N)}\rangle$ calculated with $C = 2$ and $N = 35$, are presented across a range of $\lambda = 0.40, 0.41, \ldots, 0.65$, for the states $n = 2, 3, 4$. Note that these cross sections have been calculated over a range of projectile electron energies, 0 eV to 500 eV, but are presented orthographically, obscuring this axis; effectively we present the maximum of each cross section across this range of projectile electron energies.

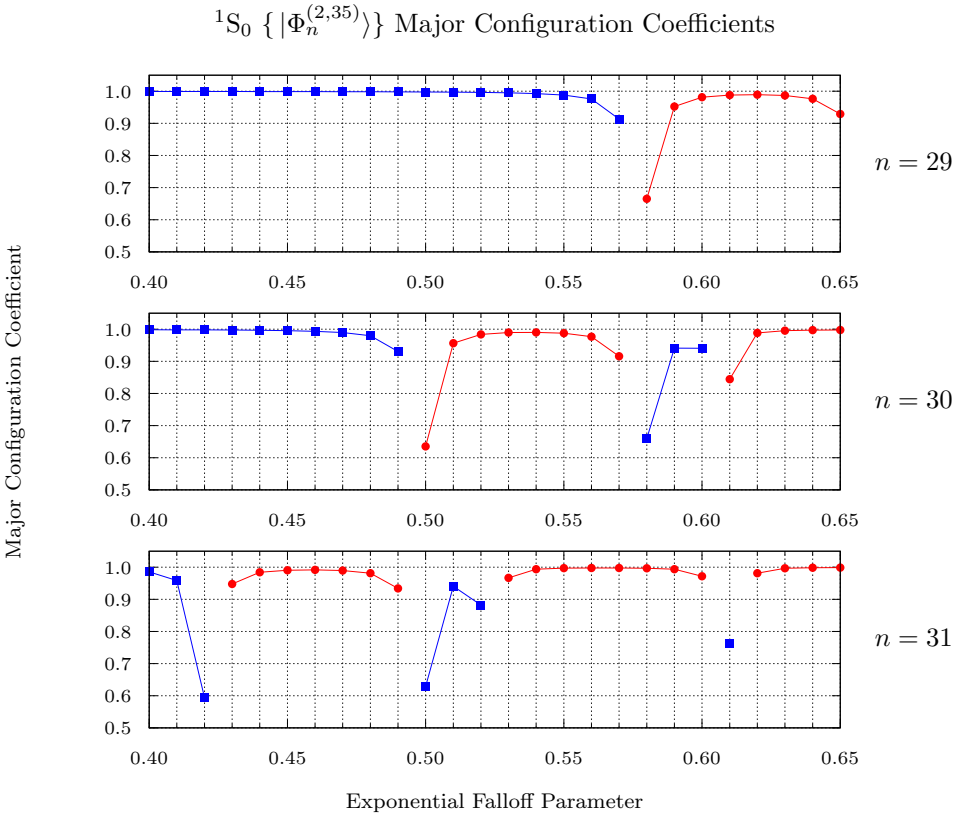

Figure 15: The major configuration coefficients of the singlet helium pseudostates, $|\Phi_n^{(C,N)}\rangle$ calculated with $C = 2$ and $N = 35$, are presented across a range of $\lambda = 0.40, 0.41, \ldots, 0.65$, for the states $n = 29, 30, 31$. Note that we present data points as being connected when they are associated with the same major configuration. Note also that blue lines indicate that the major configuration has an unexcited core state (1s), while red lines indicate an excited core state (2s).

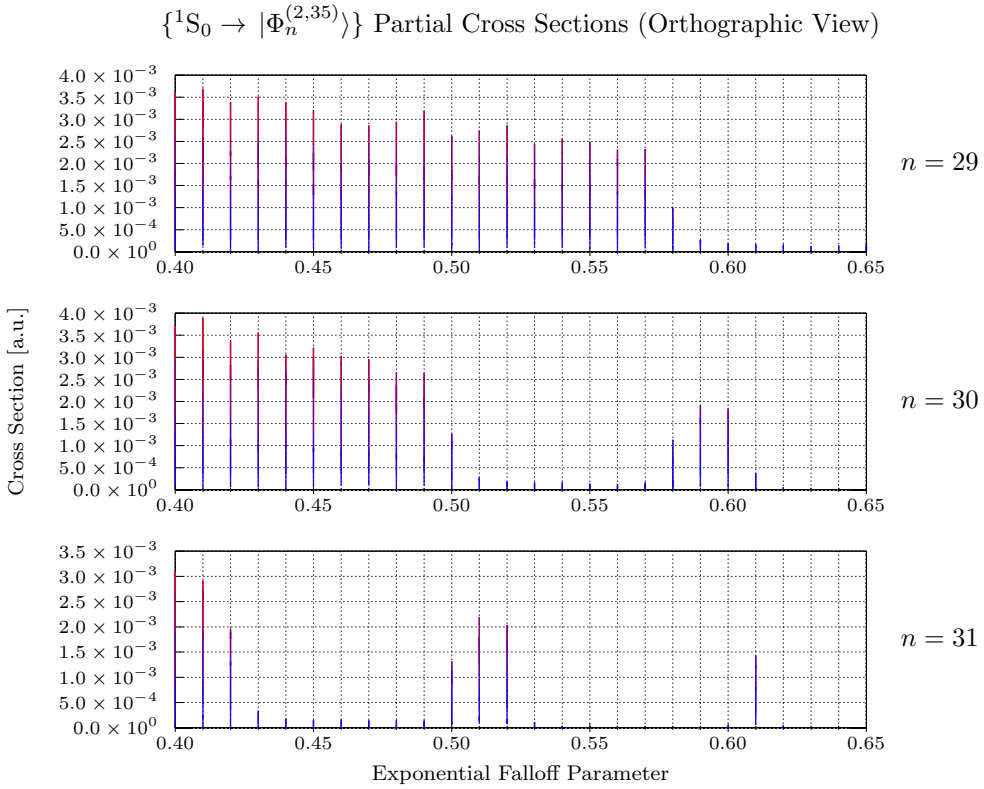

Figure 16: The partial cross sections of ground state singlet helium to the singlet pseudostates, $|\Phi_n^{(C,N)}\rangle$ calculated with $C = 2$ and $N = 35$, are presented across a range of $\lambda = 0.40, 0.41, \ldots, 0.65$, for the states $n = 29, 30, 31$. Note that these cross sections have been calculated over a range of projectile electron energies, 0 eV to 500 eV, but are presented orthographically, obscuring this axis; effectively we present the maximum of each cross section across this range of projectile electron energies.

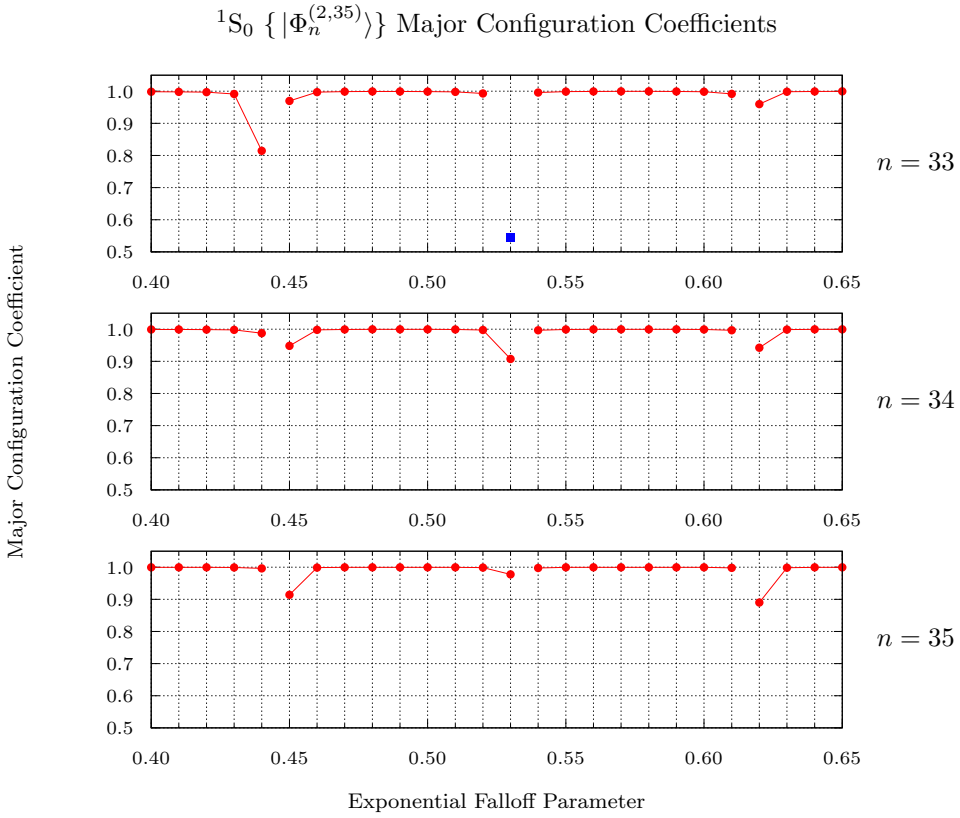

Figure 17: The major configuration coefficients of the singlet helium pseudostates, $|\Phi_n^{(C,N)}\rangle$ calculated with $C = 2$ and $N = 35$, are presented across a range of $\lambda = 0.40, 0.41, \ldots, 0.65$, for the states $n = 33, 34, 35$. Note that we present data points as being connected when they are associated with the same major configuration. Note also that blue lines indicate that the major configuration has an unexcited core state (1s), while red lines indicate an excited core state (2s).

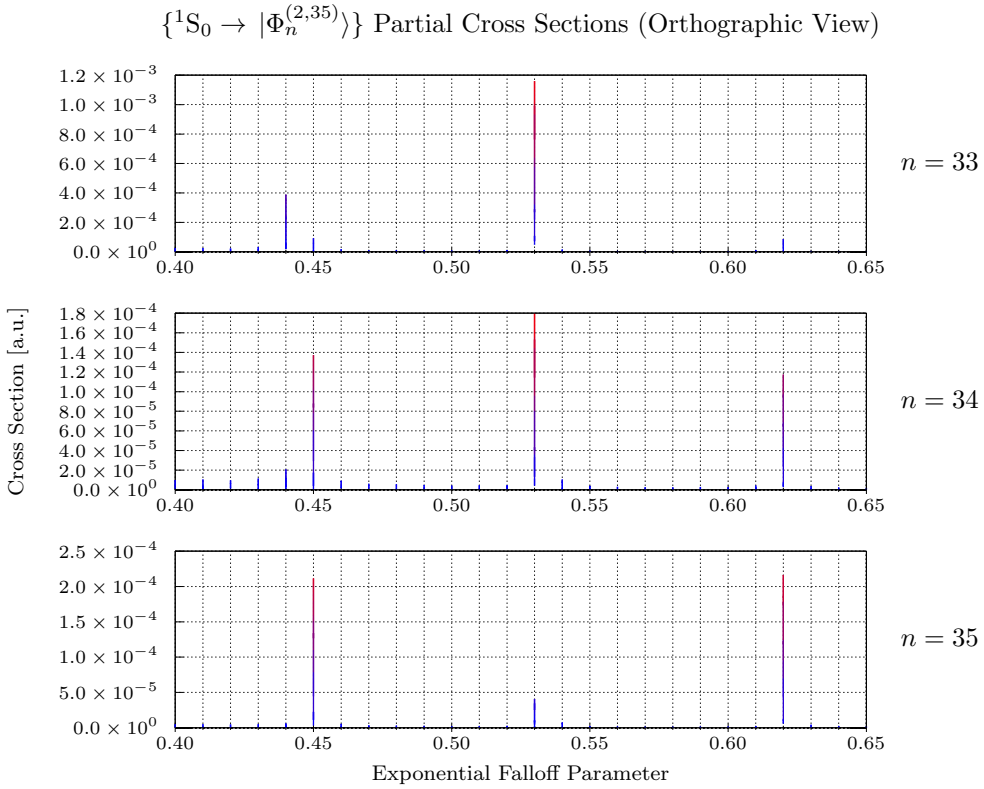

Figure 18: The partial cross sections of ground state singlet helium to the singlet pseudostates, $|\Phi_n^{(C,N)}\rangle$ calculated with $C = 2$ and $N = 35$, are presented across a range of $\lambda = 0.40, 0.41, \ldots, 0.65$, for the states $n = 33, 34, 35$. Note that these cross sections have been calculated over a range of projectile electron energies, 0 eV to 500 eV, but are presented orthographically, obscuring this axis; effectively we present the maximum of each cross section across this range of projectile electron energies.

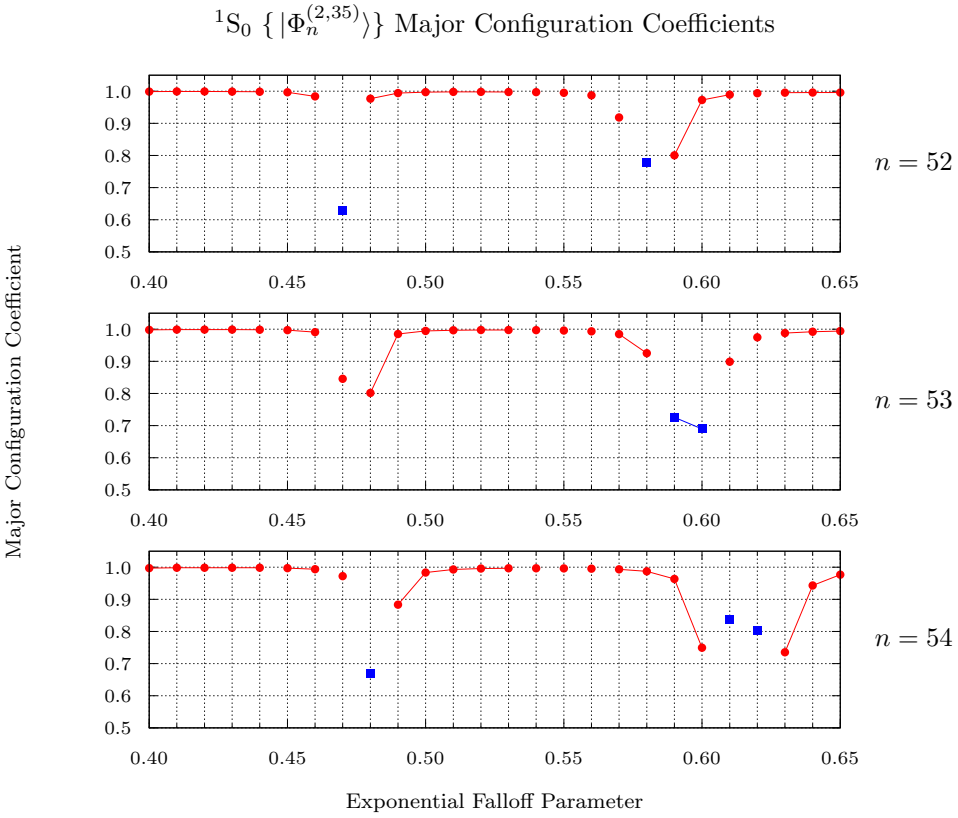

Figure 19: The major configuration coefficients of the singlet helium pseudostates, $|\Phi_n^{(C,N)}\rangle$ calculated with $C = 2$ and $N = 35$, are presented across a range of $\lambda = 0.40, 0.41, \ldots, 0.65$, for the states $n = 52, 53, 54$. Note that we present data points as being connected when they are associated with the same major configuration. Note also that blue lines indicate that the major configuration has an unexcited core state (1s), while red lines indicate an excited core state (2s).

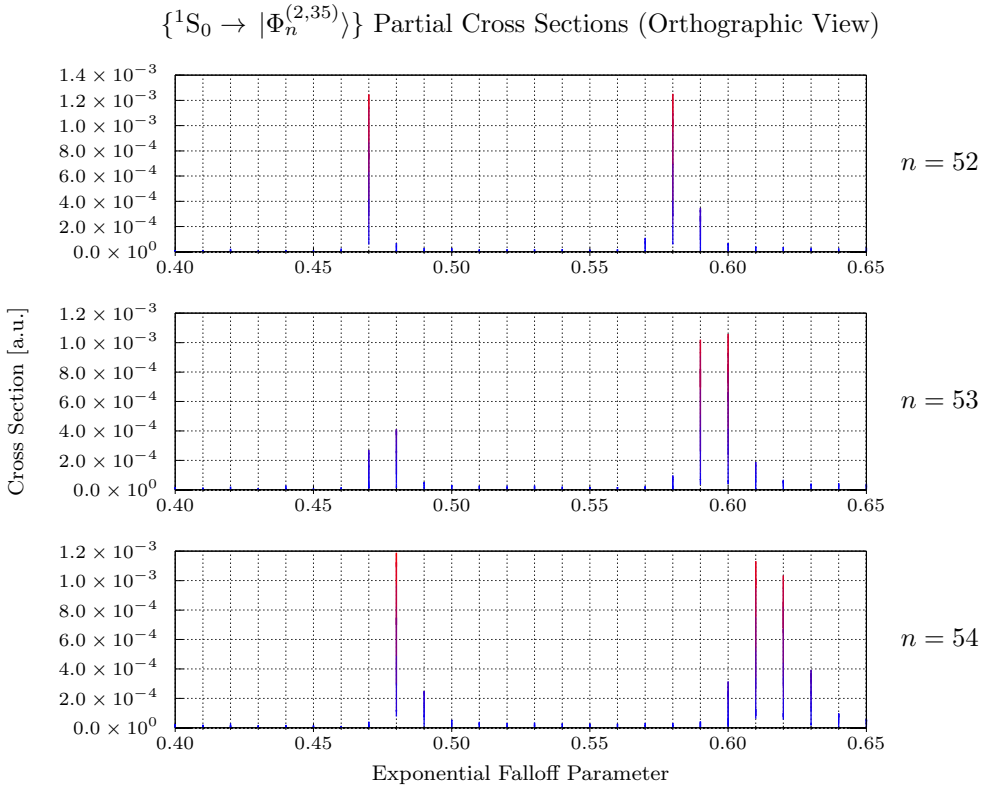

Figure 20: The partial cross sections of ground state singlet helium to the singlet pseudostates, $|\Phi_n^{(C,N)}\rangle$ calculated with $C = 2$ and $N = 35$, are presented across a range of $\lambda = 0.40, 0.41, \ldots, 0.65$, for the states $n = 52, 53, 54$. Note that these cross sections have been calculated over a range of projectile electron energies, 0 eV to 500 eV, but are presented orthographically, obscuring this axis; effectively we present the maximum of each cross section across this range of projectile electron energies.

4 Conclusions

We have sought to calculate total cross sections for electron-impact ionisation-with-excitation of helium, using the CCC method, which are in agreement with those calculated using the PECS method [22]. In this effort, we have had mixed success, being able to produce calculations which are in agreement but are not yet presentable as being issue-free calculations. However, we believe we have identified the primary cause of these issues: the calculated helium pseudostates being substantially mixed states, specifically with high-flux ionised-without-excitation continuum states mixing with low-flux doubly-excited discrete & ionised-with-excitation continuum states. The mixing of these states causes the CCC calculations to transfer a small fraction of flux from the higher magnitude ionised-without-excitation cross section, to the signficantly smaller magnitude ionised-with-excitation cross sections - causing at-times significant inaccuracies.

We are able to suggest two alternative methods of resolving these issues. The first is to develop a method by which a value for the exponential fall-off of the Laguerre basis, λ, may be determined which optimises the purity of the target configurations, yielding un-mixed target pseudostates and thus delivering ionisation-with-excitation cross sections free of interference from the ionised-without-excitation pseudostates. It is likely that an optimal value of λ would also maximise the separations between target pseudoenergies, although the question of which pseudostates should be preferentially well separated remains. The second would be to proceed with the CCC method as usual, but to create an additional set of pure target pseudostates by other means, and then to perform a basis transformation between the mixed and pure sets of target pseudostates, allowing the transition amplitudes calculated with the mixed pseudostates to yield interference-free transition amplitudes in terms of the pure pseudostates.

With the use of either of these techniques, or any other novel techniques, the application of the CCC method to the problem of calculating total cross sections for the electron-impact ionisation-with-excitation of helium may be brought into agreement with the calculations of other methodologies.

References

[1] U. Fano. Effects of configuration interaction on intensities and phase shifts. *Phys. Rev.*, 124:1866–1878, Dec 1961.

[2] Igor Bray and Andris T. Stelbovics. Convergent close-coupling calculations of electron-hydrogen scattering. *Phys. Rev. A*, 46:6995–7011, Dec 1992.

[3] Igor Bray and Andris T. Stelbovics. Calculation of the total ionization cross section and spin asymmetry in electron-hydrogen scattering from threshold to 500 ev. *Phys. Rev. Lett.*, 70:746–749, Feb 1993.

[4] Igor Bray. Close-coupling theory of ionization: Successes and failures. *Phys. Rev. Lett.*, 78:4721–4724, Jun 1997.

[5] Andris T. Stelbovics. Calculation of ionization within the close-coupling formalism. *Phys. Rev. Lett.*, 83:1570–1573, Aug 1999.

[6] Igor Bray. Convergent close-coupling method for the calculation of electron scattering on hydrogenlike targets. *Phys. Rev. A*, 49:1066–1082, Feb 1994.

[7] Igor Bray and Andris T. Stelbovics. Explicit demonstration of the convergence of the close-coupling method for a coulomb three-body problem. *Phys. Rev. Lett.*, 69:53–56, Jul 1992.

[8] Igor Bray and Andris T. Stelbovics. The convergent close-coupling method for a coulomb three-body problem. *Computer Physics Communications*, 85(1):1–17, 1995.

[9] Igor Bray. Close-coupling approach to coulomb three-body problems. *Phys. Rev. Lett.*, 89:273201, Dec 2002.

[10] Dmitry V. Fursa and Igor Bray. Calculation of electron-helium scattering. *Phys. Rev. A*, 52:1279–1297, Aug 1995.

[11] Igor Bray and Dmitry V. Fursa. Convergent close-coupling method: A "complete scattering theory"? *Phys. Rev. Lett.*, 76:2674–2677, Apr 1996.

[12] Dmitry V Fursa and Igor Bray. Convergent close-coupling calculations of electron - helium scattering. *Journal of Physics B: Atomic, Molecular and Optical Physics*, 30(4):757–785, feb 1997.

[13] Anatoli S. Kheifets and Igor Bray. Calculation of double photoionization of helium using the convergent close-coupling method. *Phys. Rev. A*, 54:R995–R997, Aug 1996.

[14] Anatoli S. Kheifets and Igor Bray. Photoionization with excitation and double photoionization of the helium isoelectronic sequence. *Phys. Rev. A*, 58:4501–4511, Dec 1998.

[15] I Bray, D V Fursa, A S Kheifets, and A T Stelbovics. Electrons and photons colliding with atoms: development and application of the convergent close-coupling method. *Journal of Physics B: Atomic, Molecular and Optical Physics*, 35(15):R117–R146, jul 2002.

[16] A. Temkin. Nonadiabatic theory of electron-hydrogen scattering. *Phys. Rev.*, 126:130–142, Apr 1962.

[17] R Poet. The exact solution for a simplified model of electron scattering by hydrogen atoms. *Journal of Physics B: Atomic and Molecular Physics*, 11(17):3081–3094, sep 1978.

[18] M. Baertschy, T. N. Rescigno, and C. W. McCurdy. Accurate amplitudes for electron-impact ionization. *Phys. Rev. A*, 64:022709, Jul 2001.

[19] Igor Bray, Dmitry V. Fursa, and Andris T. Stelbovics. Close-coupling approach to electron-impact ionization of helium. *Phys. Rev. A*, 63:040702, Mar 2001.

[20] C Plottke, P Nicol, I Bray, D V Fursa, and A T Stelbovics. Electron-impact helium double excitation within the s-wave model. *Journal of Physics B: Atomic, Molecular and Optical Physics*, 37(18):3711–3721, sep 2004.

[21] Philip L. Bartlett and Andris T. Stelbovics. Electron-helium s-wave model benchmark calculations. i. single ionization and single excitation. *Phys. Rev. A*, 81:022715, Feb 2010.

[22] Philip L. Bartlett and Andris T. Stelbovics. Electron-helium s-wave model benchmark calculations. ii. double ionization, single ionization with excitation, and double excitation. *Phys. Rev. A*, 81:022716, Feb 2010.

[23] Igor Bray. Calculation of electron scattering on atoms and ions. *Australian Journal of Physics - AUST J PHYS*, 49, 01 1996.

[24] I. Bray, C. J. Guilfoile, A. S. Kadyrov, D. V. Fursa, and A. T. Stelbovics. Ionization amplitudes in electron-hydrogen collisions. *Phys. Rev. A*, 90:022710, Aug 2014.

[25] Igor Bray and Dmitry V. Fursa. Calculation of ionization within the close-coupling formalism. *Phys. Rev. A*, 54:2991–3004, Oct 1996.